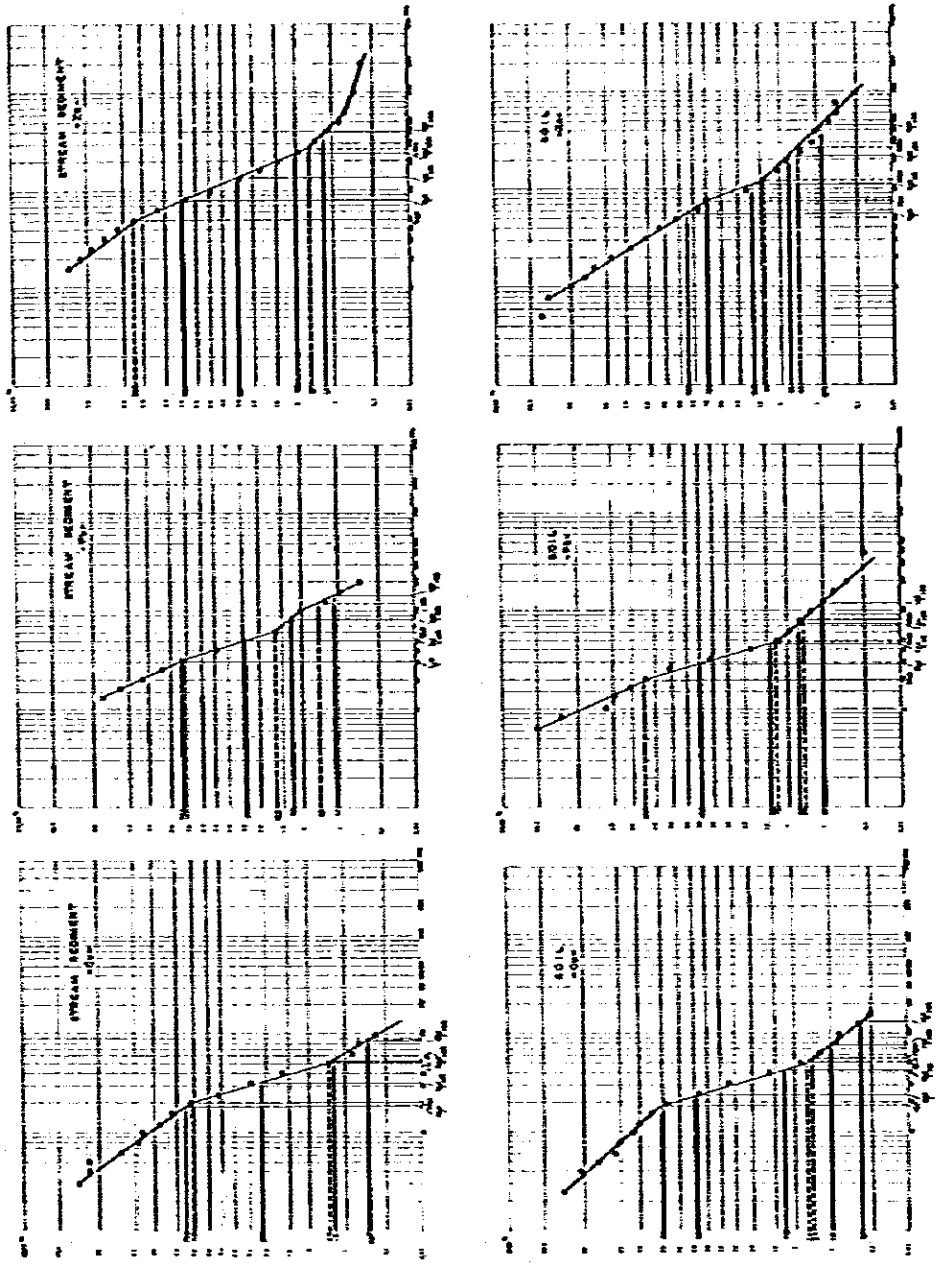


FIG. 19 CUMULATIVE FREQUENCY DISTRIBUTION — AREA - 6 —



As seen in these figures, there is no practical difference in value between two types of thresholds, so long as those of "All sample group" are concerned.

(C) The 2nd phase

General remarks: The statistical data processing in the phase-II was carried out, following nearly the same procedure with one in the phase-I. However, the nature of the data themselves in this phase was different from that in the phase-I in the following two points: All the samples treated were soil, not including streams sediment. The samples were collected in isolated seven smaller areas, most of which had been selected just around the major anomalies in the 1st phase, not being collected in larger and arbitrarily selected areas as in the phase-I.

The frequency distribution histograms and the cumulative frequency curves of each area were printed out by computer, area by area. These are attached to the section of each area's description in the phase-II report. Statistical parameters of assay values, such as mean, maximum, minimum, range, standard deviation, coefficient variance, and so forth were selected or computed. Correlation analysis of four elements were carried out. Summary of both the statistical parameters and correlation analysis are tabulated in Table-12 in this report.

In the 2nd phase, the processing was done in logarithmic scale from the beginning, without comparing it with antilogarithmic scale. A trace was mathematically treated as 0.4ppm for three elements Cu, Pb and Zn, and as 0.04ppm for Ag. The latter brought some trouble in determining threshold value as "Mean + 2 standard deviations", as mentioned in 4-4-2-(A).

Comparison of various threshold values: In the determination of the threshold values in this phase, two problems were involved: One was; Which of the two methods was more appropriate to the given situation? Another was that whether it was adequate or not, to determine the threshold in each small area separately. Both are related each other in some extent.

Simultaneous to the computation of the threshold values by "Statistical method", the patterns of the frequency distribution histogram of each area were carefully examined, and subsequently "threshold" of each element was graphically read from the cumulative frequency curve by "Lepeltier's method".

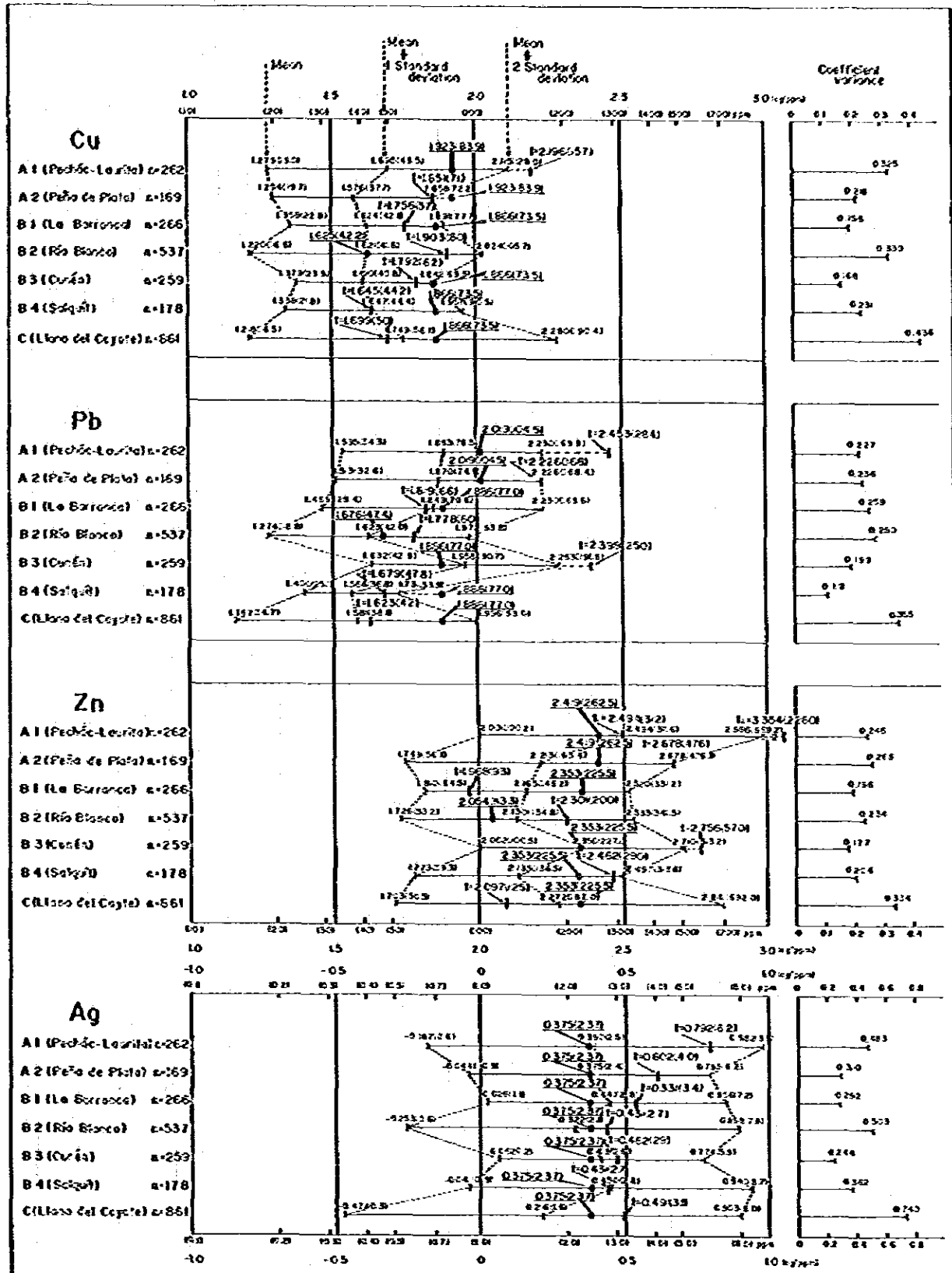
Table 12 Summary of Statistical Data of Geochemical Samples (Phase II)

All the figures are in logarithmic scale except those in parentheses which are indicated in antilogarithmic ppm values.

| Area                           | Elements | Mean (ppm)        | Standard Deviation | SD/Mean  | Mean $\pm$ 1SD    | Mean $\pm$ 2SD    | Minimum           | Maximum             | Range  | Correlation Analysis |        |        |         |         |
|--------------------------------|----------|-------------------|--------------------|----------|-------------------|-------------------|-------------------|---------------------|--------|----------------------|--------|--------|---------|---------|
|                                |          |                   |                    |          |                   |                   |                   |                     |        | Cu                   | Pb     | Zn     |         |         |
| A-1<br>Pechón-Saurica<br>n=262 | Cu       | 1.2789<br>(19.0)  | 0.4158             | 0.3231   | 2.6947<br>(49.5)  | 2.1105<br>(129.0) | 0.0000<br>(1.0)   | 3.4584<br>(2,875.0) | 3.4584 | 0.1588               | 0.1000 | 0.1000 | 0.5519  | 0.5722  |
|                                | Pb       | 1.5347<br>(34.3)  | 0.3678             | 0.2264   | 2.8873<br>(76.8)  | 2.2103<br>(165.8) | 0.4771<br>(30.0)  | 2.5837<br>(385.0)   | 2.1061 | 0.0000               | 0.6364 | 0.0000 | 0.4800  | 0.4800  |
|                                | Zn       | 1.0008<br>(100.7) | 0.4928             | 0.2663   | 2.9806<br>(96.8)  | 2.4906<br>(31.0)  | 0.5990<br>(40.0)  | 13,000.0            | 3.3802 | 1.0000               | 0.0000 | 1.0000 | 0.4730  | 0.4730  |
|                                | Ag       | 0.1872<br>(0.6)   | 0.5844             | -0.1218  | 0.3972<br>(9.6)   | 0.9816<br>(9.6)   | -1.3979<br>(0.06) | 0.9888              | 2.3847 |                      |        |        | 1.0000  | 1.0000  |
| A-2<br>Peña de Plata<br>n=187  | Cu       | 1.2942<br>(19.7)  | 0.2821             | 0.2180   | 1.5703<br>(37.7)  | 1.0044<br>(72.2)  | 0.4771<br>(3.0)   | 2.3909<br>(246.0)   | 1.9138 | 0.1976               | 0.1512 | 1.0000 | 0.5302  | 0.3945  |
|                                | Pb       | 1.5128<br>(32.6)  | 0.3568             | 0.2358   | 2.8696<br>(74.1)  | 2.2664<br>(68.4)  | 0.8021<br>(6.0)   | 3.2376<br>(1818.0)  | 2.6375 |                      |        | 1.0000 | 0.7463  | 0.5276  |
|                                | Zn       | 1.7487<br>(56.1)  | 0.4645             | 0.2656   | 2.2134<br>(163.4) | 1.6777<br>(47.6)  | 0.8004<br>(7.0)   | 3.6537<br>(2843.0)  | 2.6087 |                      |        | 1.0000 | 0.3042  | 0.3042  |
|                                | Ag       | 0.0638<br>(0.9)   | 0.6192             | -0.5708  | 0.3724<br>(2.4)   | 0.7966<br>(6.2)   | -1.3979<br>(0.06) | 0.7484<br>(5.6)     | 2.1461 |                      |        |        | 1.0000  | 1.0000  |
| B-1<br>La Derranca<br>n=266    | Cu       | 1.3576<br>(22.8)  | 0.2665             | 0.1963   | 1.9244<br>(42.1)  | 1.3795<br>(29.0)  | 0.5010<br>(2.0)   | 3.8750<br>(75.0)    | 1.5740 | 0.1376               | 0.1204 | 1.0000 | 0.2546  | 0.2155  |
|                                | Pb       | 1.4687<br>(29.4)  | 0.3804             | 0.2590   | 2.8694<br>(70.6)  | 2.4495<br>(69.6)  | 0.4771<br>(3.0)   | 3.7103<br>(372.0)   | 2.9934 | 1.0000               | 0.7994 | 1.0000 | 0.2476  | 0.2476  |
|                                | Zn       | 1.8095<br>(64.5)  | 0.3553             | 0.1964   | 2.1068<br>(46.2)  | 1.5201<br>(33.2)  | 1.0000<br>(10.0)  | 2.6963<br>(497.0)   | 1.6963 |                      |        | 1.0000 | 0.3117  | 0.3117  |
|                                | Ag       | 0.0255<br>(1.2)   | 0.4150             | 16.2745  | 0.4465<br>(2.8)   | 0.8355<br>(7.2)   | -1.3979<br>(0.06) | 0.6844<br>(6.8)     | 2.0792 |                      |        |        | 1.0000  | 1.0000  |
| B-2<br>Río Blanco<br>n=237     | Cu       | 1.2195<br>(16.4)  | 0.4023             | 0.3299   | 1.6210<br>(41.8)  | 1.0241<br>(20.2)  | 0.0000<br>(1.0)   | 2.1353<br>(163.0)   | 2.1353 | 0.1111               | 0.0847 | 1.0000 | 0.6235  | 0.6191  |
|                                | Pb       | 1.2742<br>(18.8)  | 0.3491             | 0.2709   | 1.8233<br>(42.0)  | 1.3724<br>(30.8)  | -0.3979<br>(0.6)  | 3.0791<br>(3,209.0) | 3.4771 | 1.0000               | 0.6843 | 1.0000 | 0.5446  | 0.5446  |
|                                | Zn       | 1.7260<br>(51.2)  | 0.4037             | 0.2339   | 2.1297<br>(136.8) | 1.5334<br>(34.5)  | 0.3979<br>(0.6)   | 3.4994<br>(3158.0)  | 3.8973 |                      |        | 1.0000 | 0.3117  | 0.3117  |
|                                | Ag       | 0.0254<br>(0.6)   | 0.5756             | -2.2715  | 0.3222<br>(2.1)   | 0.8978<br>(7.9)   | -1.3979<br>(0.06) | 0.9390<br>(6.1)     | 2.3570 |                      |        |        | 1.0000  | 1.0000  |
| B-3<br>Cudén<br>n=259          | Cu       | 1.3769<br>(29.9)  | 0.2316             | 0.1680   | 1.8492<br>(40.8)  | 1.4618<br>(49.5)  | 0.0000<br>(1.0)   | 2.9731<br>(94.0)    | 1.8731 | 0.1908               | 0.1270 | 1.0000 | 0.3124  | 0.2688  |
|                                | Pb       | 1.6372<br>(42.9)  | 0.3253             | 0.1993   | 1.9575<br>(40.7)  | 1.5268<br>(191.8) | 0.9342<br>(9.0)   | 3.0310<br>(1076.0)  | 2.0767 | 1.0000               | 0.6460 | 1.0000 | 0.3319  | 0.3319  |
|                                | Zn       | 1.0023<br>(100.5) | 0.3540             | 0.1768   | 1.3562<br>(227.1) | 1.1203<br>(131.2) | 1.0424<br>(11.0)  | 3.4529<br>(1,628.0) | 2.1133 |                      |        | 1.0000 | 0.3806  | 0.3806  |
|                                | Ag       | 0.0621<br>(1.2)   | 0.3560             | 5.7354   | 0.6181<br>(2.6)   | 0.7741<br>(5.9)   | -1.3979<br>(0.06) | 0.7604<br>(5.5)     | 2.1187 |                      |        |        | 1.0000  | 1.0000  |
| B-4<br>Salquell<br>n=170       | Cu       | 1.3378<br>(21.8)  | 0.3094             | 0.2313   | 1.6672<br>(46.4)  | 1.1906<br>(30.3)  | -0.3979<br>(0.6)  | 1.8921<br>(78.0)    | 2.2900 | 0.3225               | 0.1423 | 1.0000 | 0.4660  | 0.3726  |
|                                | Pb       | 1.4602<br>(24.1)  | 0.1655             | 0.1182   | 1.9353<br>(36.9)  | 1.7312<br>(59.9)  | 0.8451<br>(7.0)   | 2.0253<br>(106.0)   | 1.1802 | 1.0000               | 0.2816 | 1.0000 | 0.1349  | 0.1349  |
|                                | Zn       | 1.7734<br>(59.3)  | 0.3616             | 0.2039   | 2.1350<br>(136.5) | 1.6956<br>(31.4)  | 0.9031<br>(8.0)   | 2.6253<br>(422.0)   | 1.7222 |                      |        | 1.0000 | -0.1054 | -0.1054 |
|                                | Ag       | 0.0422<br>(0.9)   | 0.4008             | -11.9176 | 0.4666<br>(2.8)   | 0.9404<br>(8.7)   | -1.3979<br>(0.06) | 0.9001<br>(3.2)     | 1.9011 |                      |        |        | 1.0000  | 1.0000  |
| C<br>Llano del Coyote<br>n=861 | Cu       | 1.2175<br>(16.5)  | 0.3311             | 0.4362   | 1.7489<br>(56.1)  | 1.2797<br>(100.6) | -0.3979<br>(0.6)  | 3.2896<br>(1848.0)  | 1.6875 | 0.0877               | 0.0684 | 1.0000 | 0.6386  | 0.2608  |
|                                | Pb       | 1.1668<br>(14.7)  | 0.4146             | 0.5552   | 1.5812<br>(38.1)  | 1.1956<br>(99.0)  | -0.3979<br>(0.6)  | 3.4530<br>(2817.0)  | 2.8838 | 1.0000               | 0.6386 | 1.0000 | 0.5894  | 0.5894  |
|                                | Zn       | 1.7020<br>(50.5)  | 0.5690             | 0.3361   | 2.1715<br>(137.0) | 1.8409<br>(69.2)  | -0.3979<br>(0.6)  | 3.4618<br>(402.0)   | 4.2392 |                      |        | 1.0000 | 0.6410  | 0.6410  |
|                                | Ag       | 0.0470<br>(0.3)   | 0.4865             | -1.4599  | 0.2162<br>(1.6)   | 0.9031<br>(8.0)   | -1.3979<br>(0.06) | 0.9129<br>(6.5)     | 2.7188 |                      |        |        | 1.0000  | 1.0000  |

\*1 "trace" is treated as 0.4ppm for Cu, Pb, and Zn and 0.04ppm for Ag respectively, for the conversion of antilogarithmic ppm values.

Fig. 20 Means - Standard Deviations - Thresholds



I: Threshold graphically read  
 a: Threshold finally adopted

Table-13 Summary of Threshold value (Phase II)

| Area | Metal | Frequency Distribution pattern. |    |    | Cumulative Frequency Distribution Pattern | Abscissa of Max of 2.5% 2SD (level) ppm | Breaking Point |          |          |                           | Mean Value finally Adopted (ppm) | Basis of Calculation for Mean |   |
|------|-------|---------------------------------|----|----|---|---|----------------|----------|----------|---------------------------|----------------------------------|-------------------------------|---|
|      |       | Cu                              | Pb | Zn |   |   | B1 (ppm)       | B2 (ppm) | B3 (ppm) | T' Graphically read (ppm) |                                  |                               |   |
| A-1  | Cu    |                                 |    |    |   | 230                                     | 129.0          | 13       | 126      | 200                       | 157                              | 83.9                          | Mean+2SD from 695 Samples from Area-A, 1976 |
|      | Pb    |                                 |    |    |   | 302                                     | 169.9          | 13       | 216      | 347                       | 284                              | 104.5                         |   |
|      | Zn    |                                 |    |    |   | 2260                                    | 969.2          | 105      | 1700     | 3162                      | 2260                             | 262.5                         |   |
|      | Ag    |                                 |    |    |   | 6.2                                     | 9.6            | 1.1      | 5.0      | 7.9                       | 5.2                              | 2.37                          | All 77 Samples                              |
| A-2  | Cu    |                                 |    |    |   | 71                                      | 72.2           |          |          |                           | 70.9                             | 83.9                          | Mean+2SD from 695 Samples from Area-A, 1976 |
|      | Pb    |                                 |    |    |   | 290                                     | 268.4          | 120      | 210      |                           | 168.4                            | 104.5                         |   |
|      | Zn    |                                 |    |    |   | 800                                     | 476.1          | 370      | 780      |                           | 476.1                            | 262.5                         |   |
|      | Ag    |                                 |    |    |   | 4.0                                     | 6.2            |          |          |                           | 4.0                              | 2.37                          | All 77 Samples                              |
| B-1  | Cu    |                                 |    |    |   | 57                                      | 77.7           | 3.3      | 21.0     |                           | 57                               | 73.5                          | Mean+2SD from 872 Samples from Area-B, 1976 |
|      | Pb    |                                 |    |    |   | 192                                     | 169.6          | 38       | 114      |                           | 66                               | 77.0                          |   |
|      | Zn    |                                 |    |    |   | 300                                     | 331.2          | 17.8     | 70       | 122                       | 93                               | 225.5                         |   |
|      | Ag    |                                 |    |    |   | 3.4                                     | 7.2            | 0.62     |          |                           | 3.4                              | 2.37                          | All 77 Samples                              |
| B-2  | Cu    |                                 |    |    |   | 80                                      | 105.7          | 22       |          |                           | 80                               | 42.2                          | Mean+1SD from 372 Samples from Area-B, 1976 |
|      | Pb    |                                 |    |    |   | 94                                      | 93.8           | 60       |          |                           | 60                               | 47.4                          |   |
|      | Zn    |                                 |    |    |   | 300                                     | 341.5          | 31       | 200      |                           | 200                              | 113.3                         |   |
|      | Ag    |                                 |    |    |   | 2.7                                     | 7.9            | 1.4      | 33       |                           | 2.7                              | 2.37                          | All 77 Samples                              |
| B-3  | Cu    |                                 |    |    |   | 62                                      | 69.5           | 17       |          |                           | 62                               | 73.5                          | Mean+2SD from 872 Samples from Area-B, 1976 |
|      | Pb    |                                 |    |    |   | 358                                     | 191.8          | 35       | 180      | 358                       | 250                              | 77.0                          |   |
|      | Zn    |                                 |    |    |   | 570                                     | 513.2          | 650      |          |                           | 570                              | 225.5                         |   |
|      | Ag    |                                 |    |    |   | 2.9                                     | 5.9            | 0.9      |          |                           | 2.9                              | 2.37                          | All 77 Samples                              |
| B-4  | Cu    |                                 |    |    |   | 52.0                                    | 90.5           | 18.6     | 44.2     |                           | 44.2                             | 73.5                          | Mean+2SD from 872 Samples from Area-B, 1976 |
|      | Pb    |                                 |    |    |   | 48                                      | 53.9           | 14.1     | 18.8     |                           | 47.8                             | 77.0                          |   |
|      | Zn    |                                 |    |    |   | 290                                     | 313.8          | 22.2     | 41.9     | 288                       | 290                              | 225.5                         |   |
|      | Ag    |                                 |    |    |   | 2.7                                     | 8.7            | 1.7      |          |                           | 2.7                              | 2.37                          | All 77 Samples                              |
| C    | Cu    |                                 |    |    |   | 210                                     | 190.4          | 50       |          |                           | 50                               | 73.5                          | Mean+2SD from 872 Samples from Area-B, 1976 |
|      | Pb    |                                 |    |    |   | 100                                     | 99.0           | 42       |          |                           | 42                               | 77.0                          |   |
|      | Zn    |                                 |    |    |   | 1080                                    | 692.0          | 125      |          |                           | 125                              | 225.5                         |   |
|      | Ag    |                                 |    |    |   | 3.3                                     | 8.0            | 0.7      |          |                           | 3.1                              | 2.37                          | All 77 Samples                              |

T' : Threshold  
 o : Threshold graphically read  
 + : Threshold finally adopted

Two types of the "threshold values" were compared and examined.

However, in conclusion, we decided not to use both the threshold values above mentioned, but to use the threshold values of "All sample groups" of the 1st phase by "Statistical method". The reasons are as follows: (1) The project areas of the 2nd phase were selected mainly around geochemical anomalies of the 1st phase, and, therefore, areas of them are limited and small (mostly 20 to 50 sq.km). Number of samples within an area is consequently small (150 to 270 except B-2, and C). From these conditions, it was anticipated that the ratio of the mineralized population to the background population would extremely vary area by area, and that there might be an area where the population was wholly affected by mineralization. However, in fact, we found it very difficult to distinguish these two populations by "Lepeltier's method" in most areas, as there were several breaking points observed on a single cumulative frequency curve. "Statistical method" is neither applicable for such a population as above, as the method is based on the assumption that the deviation from lognormal is small. (2) It is inconvenient for the comparison of the different areas to adopt extremely different threshold values area by area.

**Threshold values finally adopted:** After having compared various thresholds as mentioned above, we decided to adopt the following ones as the threshold values: "Mean + 2 standard deviations" calculated from "All Sample group" in the 1st phase was, as a rule, adopted for Cu, Pb and Zn. "Mean + 1 standard deviation" calculated from all the samples collected in the phase -II was adopted for Ag, as no Ag assay was made in the 1st phase.

These finally adopted thresholds values are shown in Table-13 as well as the threshold value by "Lepeltier's method" and "Mean + 2 standard deviations" of each area. In this table, threshold values by "Lepeltier's method" are denoted as "T graphically read".

In Area B-2, "Mean + 1 standard deviation" was adopted instead of two standard deviations, by way of trial, for the three elements. The reasons were as follows: Little anomalous value would have been picked up in this area, if a normal 2 standard deviations had been adopted, as all the assay values here were fairly low. However, we considered at that time that much less Cu and Zn might remain in soil in this area than in other areas where carbonate rocks occurred. Because, the leached capping is well developed, and there are less carbonate rocks in the area. Therefore, 1 standard deviation was tentatively adopted for this particular area. This also, at the time, aimed at to reveal the relationship between the distribution of the elements and igneous rocks. Nevertheless, anomalies delineated by 2 standard deviations are shown in PL-6 of this report, for better comparison with other areas on the same basis.

For Ag, "Mean + 1 standard deviation" calculated from all the 2,532 samples in the 2nd phase was used as a common threshold for all the seven areas. There reason why "2 standard deviations" was not adopted, is because there was few sample that exceeded this value. This may be attributed to the fact that there were many samples whose Ag values were "trace" and it was mathematically treated as 0.04ppm so that the standard deviation in logarithmic scale apparently became large.

**Discussion:** In the present project, our comparison of various thresholds finally resulted in to use "Mean + 2 standard deviations" of "All sample group" of Phase-I as the thresholds through out two phases. However, we still consider that to try "Lepeltier's method" is not futile: Should we distinguish the "mineralized population" by a breaking point, we shall utilize it as a threshold. Even if not, we shall be able to obtain the knowledge on the nature of a population through practicing the method.

In the present project, the rolling mean analysis was not applied for the determination of the threshold values. Nevertheless, it may be reasonable to apply this technique for the determination of the threshold values, especially in the reconnaissance stage. The procedure may be suggested as follows: To construct the surface showing "rolling mean + 2 standard deviations calculated from all the samples falling in that search area". To define "anomaly" or "anomalous area" as an area where the residual (of assayed value less assigned value of that point on the calculated surface) is positive.

#### 4-4-3 Determination and presentation of anomalies

Geochemical anomaly was extracted using the threshold values defined by "Statistical method" discussed above. Definition of an anomaly in each phase and the presentation of anomalies are described below.

##### (A) 1st phase

**Definition:** "The anomalous areas have been delineated as the places where several "anomalous values"(the value that exceeds "mean + 2 standard deviations") are relatively crowded within a comparatively large area. Sporadically distributed high values within a comparatively large area, if any, are not considered as an anomalous area, even though the values themselves are relatively high. (p-86 in Phase-I report).

**Presentation of anomalies:** Selected anomalies(anomalous areas) are summarized in Table C-17 in the Phase-I report, and it is taken in this report as Table-14.

Anomalies in Area-A were shown in PL-22 through 27 attached to Phase-I report, and those in Area-B were shown in PL-35 through 46 of the same report. In order to select the follow-up target areas, these major anomalies were examined and compared with other factors, and were compiled in PL-34 and -53 in Phase-I report. These maps were revised with the results of the phase-II operations, and are attached to this report as PL-5 and -6.

**Selection of target areas for Phase-II:** The target areas were selected from the anomalies, by integrating the result of the rolling mean analysis, geological factors, and other factors. This will be discussed in 4-4-6.

##### (B) 2nd phase

**Definition:** "An anomaly is defined here as an area in which plural sample sites, whose assay values exceed the threshold value, are adjacently existed, and the continuation among them is inferred both geologically and geographically" (p.53 in Phase-II report). Furthermore, eleven major anomalies were selected, after the extents and assay values of the anomalies, geological factors, and various other factors had been taken into consideration. In Area-C, where grid sampling was practiced, an anomaly was delineated by the isograde line whose value is approximately the same to the threshold value.



Table -14 Anomalous Areas Chosen Statistically (Phase I)

| No. | Area | Name of Anomaly  | Location  |      |      | Type of Samples | Element | Approximate Area (km x km) | Nos. of Anomalous Samples |           |                 | Max. of Anomalous Values (ppm) |           | Remarks     |
|-----|------|------------------|-----------|------|------|-----------------|---------|----------------------------|---------------------------|-----------|-----------------|--------------------------------|-----------|-------------|
|     |      |                  | Quad. No. | X    | Y    |                 |         |                            | 1st Anom.                 | 2nd Anom. | Intermed. Anom. | 1st Anom.                      | 2nd Anom. |             |
|     |      | Laurita          | 1863-1    | 52.5 | 54.2 | Sed.            | Pb      | 0.5x1.5                    | 1                         | 1         | 1               | 5,333                          | 142       | Predominant |
|     |      | "                | "         | "    | "    | "               | Zn      | 0.5x2.0                    | 1                         | 2         | 1               | 1,333                          | 328       | "           |
|     |      | Peché            | "         | 48.2 | 52.8 | "               | Pb      | 1.0x3.0                    | 0                         | 1         | 4               | -                              | 136       | "           |
|     |      | "                | "         | 46.4 | 52.3 | "               | Zn      | 1.0x6.0                    | 2                         | 1         | 5               | 864                            | 318       | Predominant |
|     |      | "                | "         | 48.0 | 53.0 | Soil            | Pb      | 1.5x4.5                    | 2                         | 4         | 13              | 218                            | 136       | "           |
|     |      | "                | "         | "    | "    | "               | Zn      | 1.5x3.5                    | 6                         | 5         | 15              | 5,882                          | 591       | "           |
|     | A    | Cerro Bobí       | 1963-3    | 62.7 | 49.6 | Sed.            | Cu      | 1.0x1.0                    | 2                         | 2         | 4               | 1,208                          | 167       | "           |
|     |      | "                | "         | "    | "    | "               | Pb      | 0.5x0.5                    | 0                         | 1         | 2               | -                              | 136       | "           |
|     |      | "                | "         | "    | "    | "               | Zn      | 0.5x1.0                    | 0                         | 2         | 2               | -                              | 250       | "           |
|     |      | Nuca Atzam       | "         | 71.0 | 49.0 | "               | Cu      | 0.5x1.5                    | 0                         | 0         | 4               | -                              | -         | "           |
|     |      | Chibachen        | "         | 78.5 | 46.5 | Soil            | Zn      | 1.0x2.0                    | 0                         | 1         | 5               | -                              | 406       | "           |
|     |      | Quiquil          | "         | 77.0 | 44.0 | "               | "       | 1.0x1.0                    | 0                         | 0         | 3               | -                              | -         | "           |
|     |      | Jueup            | 1863-2    | 48.5 | 44.0 | "               | Pb      | 0.5x2.0                    | 0                         | 0         | 4               | -                              | -         | "           |
|     |      | "                | "         | "    | "    | "               | Zn      | 0.5x3.0                    | 0                         | 1         | 4               | -                              | 380       | "           |
|     |      | La Barranca      | 1962-3    | 74.5 | 97.3 | Sed.            | Pb      | 1.0x6.5                    | 1                         | 2         | 8               | 156                            | 126       | Predominant |
|     |      | Río Acul         | 1962-2    | 94.8 | 2.0  | "               | "       | x1.5                       | 0                         | 1         | 3               | -                              | 100       | "           |
|     |      | "                | "         | 94.5 | 3.0  | "               | Zn      | x4.0                       | 0                         | 4         | 5               | -                              | 273       | "           |
|     |      | Río Chuleto      | "         | 97.5 | 3.0  | "               | "       | x1.0                       | 2                         | 1         | 0               | 877                            | 400       | "           |
|     |      | Río Chiquatuf    | "         | 99.5 | 97.0 | "               | Cu      | x2.5                       | 0                         | 0         | 9               | -                              | -         | "           |
|     |      | Río Azul         | "         | 2.3  | 6.5  | "               | Pb      | x3.0                       | 0                         | 2         | 5               | -                              | 122       | "           |
|     | B    | Cundín           | "         | 12.5 | 97.0 | Soil            | "       | 1.0x2.0                    | 1                         | 2         | 2               | 500                            | 89        | Predominant |
|     |      | "                | "         | "    | "    | "               | Zn      | 1.5x2.0                    | 3                         | 4         | 0               | 1,000                          | 440       | "           |
|     |      | Río Cobanero     | 2062-3    | 16.3 | "    | Sed.            | "       | x1.0                       | 1                         | 1         | 0               | -                              | 257       | "           |
|     |      | Quebrada Lutal   | "         | 19.3 | 97.6 | "               | Pb      | x2.0                       | 0                         | 3         | 1               | -                              | 117       | "           |
|     |      | "                | "         | "    | "    | "               | Zn      | x2.0                       | 0                         | 0         | 4               | -                              | -         | "           |
|     |      | Quebrada Xecanas | "         | 22.0 | 97.5 | "               | Pb      | x1.5                       | 0                         | 2         | 3               | -                              | 130       | "           |
|     |      | "                | "         | "    | "    | "               | Zn      | x1.5                       | 0                         | 0         | 4               | -                              | -         | "           |

Table 15 Summary of Major Geochemical Anomalies (Phase II)

| No. | Area | Name of Anomaly             | IGN Quad-<br>rangle map                               | UTM *<br>Coordinates |      | Element              | Area<br>(km <sup>2</sup> )                           | Max. Value<br>in Anom.<br>Area (ppm)   | Mean Value<br>in Anom.<br>Area (ppm)                    | Remarks |
|-----|------|-----------------------------|---|----------------------|------|----------------------|--|--|---|---------|
|     |      |                             |   | X                    | Y    |                      |  |  |   |         |
| 1   | A-1  | Peñasco<br>Pocumal          | 1863-1<br>(Ocentó)                                    | 52.7                 | 54.7 | Cu<br>Pb<br>Zn<br>Ag | 3.0X0.7<br>Cu 2,875<br>Pb 168<br>Zn 12,000<br>Ag 9.7 | Cu 678<br>Pb 140<br>Zn 2,117<br>Ag 9.7 | Area surrounding<br>Laurita old work                    |         |
| 2   | A-2  | East of<br>Saclecán         | 1963-3<br>(Barillas)                                  | 78.3                 | 45.2 | Pb<br>Zn<br>Ag       | 1.0X1.5<br>Pb 454<br>Zn 1,091<br>Ag 5.6              | Pb 241<br>Zn 651<br>Ag 3.9             | Between Saclecán out crop<br>and Peña de Plata old work |         |
| 3   | B-1  | South-west of<br>Cantzela   | 1962-3<br>(Chiantla)                                  | 74.5                 | 98.5 | Pb<br>Zn             | 1.3X1.0<br>Pb 226<br>Zn 306                          | Pb 127<br>Zn 259                       |   |         |
| 4   | B-2  | South of<br>La Estancia     | 1962-3<br>(Chiantla)                                  | 86.3                 | 96.2 | Cu<br>Pb<br>Zn<br>Ag | 1.0X0.3<br>Cu 130<br>Pb 207<br>Zn 3,158<br>Ag 4.8    | Cu 88<br>Pb 171<br>Zn 1,965<br>Ag 3.6  | Anomaly delineated by<br>Mean + 1SD                     |         |
| 5   | B-2  | Xetzaiel                    | 1961-1<br>(Sacapulas)                                 | 97.3                 | 91.7 | Cu<br>Pb<br>Zn       | 0.7X0.2<br>Cu 127<br>Pb 1,200<br>Zn 635              | Cu 95<br>Pb 722<br>Zn 589              | "   |         |
| 6   | B-2  | North-west of<br>Sacapulas  | 1961-1<br>(Sacapulas)                                 | 102.7                | 92.0 | Cu<br>Pb<br>Zn       | 1.0X3.0<br>Cu 112<br>Pb 87<br>Zn 148                 | Cu 60<br>Pb 72<br>Zn 135               | "   |         |
| 7   | B-3  | Cuñen                       | 1962-2<br>2062-3<br>Nebaj<br>(Tz'ajá)                 | 117.0                | 96.5 | Pb<br>Zn             | 1.0X1.5<br>Pb 1,074<br>Zn 1,428                      | Pb 178<br>Zn 415                       | Along chochal limestone                                 |         |
| 8   | C    | Llano del<br>Coyote<br>W24  | 1961-4<br>1961-1<br>(Huehueten-<br>ango<br>Sacapulas) | 87.9                 | 95.3 | Cu<br>Pb<br>Zn<br>Ag | 0.7X0.3<br>Cu 168<br>Pb 2,857<br>Zn 2,283<br>Ag 3.9  | Cu 122<br>Pb 1,089<br>Zn 757<br>Ag 3.3 |   |         |
| 9   | C    | Llano del Coyote<br>W4      | 1961-1<br>(Sacapulas)                                 | 89.9                 | 94.8 | Cu<br>Zn             | 1.0X0.2<br>Cu 295<br>Zn 2,444                        | Cu 159<br>Zn 884                       |   |         |
| 10  | C    | Llano del Coyote<br>W18-E18 | 1961-1<br>(Sacapulas)                                 | 90.1                 | 94.1 | Cu<br>Pb<br>Zn<br>Ag | 3.6X0.2<br>Cu 429<br>Pb 195<br>Zn 6,947<br>Ag 4.0    | Cu 167<br>Pb 118<br>Zn 1,025<br>Ag 3.2 |   |         |
| 11  | C    | Llano del Coyote<br>E24     | 1961-1<br>(Sacapulas)                                 | 92.0                 | 92.7 | Cu<br>Pb<br>Zn<br>Ag | 1.2X0.3<br>Cu 574<br>Pb 275<br>Zn 6,900<br>Ag 5.5    | Cu 224<br>Pb 147<br>Zn 1,228<br>Ag 3.8 |   |         |

\* Coordinates read at approximate center

Presentation: The limits of the anomalies in all the areas were outlined in maps showing Geochemical Result, the plate Nos. of which are described in 4-3 of this report.

The eleven major anomalies mentioned above are listed in Table-15 in this report, and are shown in PL-5 and -6 attached to this report.

#### 4-4-4 Rolling mean analysis

Rolling mean analysis was carried out in the 1st phase. The rolling mean analysis or weighted moving average analysis may be regarded as the application of the one-dimensional smoothing technique for areally distributed data (Nichol et al.; 1969).

When it is applied to the interpretation of geochemical data, the regional trend in the geographical distribution of geochemical parameters can be obtained. The parameters usually include assay values, their standard deviations, ratios of assay values of different elements, and so forth. In the rolling mean analysis, all the anomalous values and/or noises are smoothed regardless of their causes, though the causes may comprise mineralization, existence of various geological units that have backgrounds of different levels, and many other factors. Therefore, the surface that is constructed by the rolling mean can be said to stand for roughly the "background" of the parameter. From this nature, the technique is helpful on interpreting the geochemical data in such cases as follows: (1) When a population cannot properly be subdivided for eliminating the effects of noises, due to lack of geological and/or other informations. (2) When iso-"grade" contours can hardly be drawn from the plots of "raw" values, due to lack of number of samples and/or strong fluctuation of the values.

The rolling mean analysis has similar nature with trend surface analysis, but the latter generally show worse fitness with the actually measured values than the former. Therefore we believe that the rolling mean analysis is more adequate than the trend surface analysis, when there are a fairly large number of samples in the area. Nevertheless, the rolling mean analysis also has an inherent demerit that there is always geographical discrepancy between the areas of high rolling mean values and actual sample points of high values. It is another problem in the method how to decide the dimension of a search area; if the search area is decided larger, the distribution of the calculated values will become smoother,

but the discrepancy between calculated values and actual ones becomes larger. On the contrary, if the search area is smaller, blank area ( an area without assigned value) will become larger and the general trend becomes obscured, though the discrepancy decreases.

The rolling mean analysis was applied in the Phase-I, as it was the phase of reconnaissance: In the phase, it is usually required to reveal the regional relationship between geological factors and distribution of indicator elements as well as to locate anomalous areas, though enough geological information is not available as yet, and the sample spacing is considerably wider. In the present project, following three parameters were computed and printed out: (1) Geometrical mean of assay values (Cu, Pb and Zn) in a search area. (2) Standard deviation of the assay values falling within that area. (3) Ratios of means of any two elements of the three (Pb/Cu, Zn/Cu, and Zn/Pb) in the area.

The search area was decided rather arbitrarily as 10km by 10km in accordance with the 10 UTM grids in an ICN quadrangle map. A 90% overlap of successive portions of the search area was selected, that is to say, the search area was moved on one grid-spacing in the ICN maps along the coordinate lines both in E-W and N-S directions. Computed values were plotted at the center of the area.

The analysis was carried out for both stream sediments and soil. However, only the maps for soil are attached to the Phase-I report to avoid duplication, because the stream sediments were sampled on much wider spacing than soil in geographically restricted areas, though they indicated nearly the same tendency as soil.

**Rolling mean:** Mean of the assay values of all the samples that fall within a search area was computed in logarithmic scale, and its antilogarithmic value was plotted at the center of the search area. These search areas were successively moved with a 90% overlap as mentioned above. The procedures were carried out by computer. Isograde contour lines were manually drawn.

The results were shown in 1/100,000 scale maps; PL-28 through 30 for Area-A, and PL-47 through 49 for Area-B in the Phase-I report. The areas of high rolling mean were tabulated in Table C-18 in the same report. A high(rolling) mean value may signify either there are high background parts, or there are any mineralized parts within the search area.

However, as pointed out in the previous pages, there is geographical discrepancy between a high-rolling mean area and the actual sample sites where the assay values are high. Generally, the discrepancy is particularly conspicuous near the periphery of the sampled area.

In Area-A, a higher Cu part is observed at the southeastern corner, and a higher Pb-Zn part near the northwestern corner. The area to which the former is attributed was selected as Area A-2 for the follow-up target in the Phase-II, after other factors had been taken into consideration. The area to which the latter is attributed was likewise selected as Area A-1.

In Area-B, a Pb-Zn high is observed between Sacapulas and Cunén near the southeastern corner of the area, and three small island-like Cu highs are recognized in a zone that diagonally crosses the area in NW-SE direction. The areas that may have caused the former were selected as Area B-2 and B-3 for the follow-up, and the area that may have caused the latter was selected as B-4, respectively.

**Standard deviation:** Standard deviation was calculated from the assay values of all the samples falling within a search area, and plotted at the center of the area. The contour maps were also prepared. All these procedures are the same with those of the rolling mean.

The results of Area-A were shown in PL-31 through 33 of the Phase-I report, and those of Area-B were in PL-50 through 52, respectively. The areas of high standard deviation were tabulated in Table C-19 in the same report.

A high standard deviation in the rolling mean analysis signifies that there is high geochemical relief within that search area, and may be related to complexities of the geology or secondary environment or to mineralization (Nichol, et al.; 1969).

In Area-A, a standard deviation high of Cu and Zn is observed around Cerro Bobí, and a high of Pb is recognized at the northwestern corner of the area, which is attributed to the mineralization in the Pechac-Laurita area. The former was investigated in more detail during the Phase-I, and the area surrounding the Pechac-Laurita prospect was covered by the follow-up in the Phase-II as Area A-1. No prominent standard deviation high is present in the proximity of Area A-2 of the Phase-II.

In Area-B standard deviation highs are observed in following places; Cu and Zn around Llano del Coyote, Pb at the southwestern part of the area near La Barranca, and Pb and Zn between Sacapulas and Cunén in the southeastern part of the area. All of these were covered by the follow-up works in the Phase-II, as Areas, -C, B-2, B-3 and B-1, respectively. However, no conspicuous high is seen in the proximity of Salquil, though B-4 in the Phase-II was located in this part.

**Geochemical zoning (Ratios of elements):** The ratios between any two of three elements (Pb/Cu, Zn/Cu, and Zn/Pb) were computed from the means of each search area, and were plotted. Contours were drawn manually in 1/100,000 maps. The procedures are the same with those of rolling mean and standard deviation.

The reason why we tried this, is because we had anticipated there might be any tendency in the assay values of geochemical samples that reflected the zonal arrangement of metallic elements caused by mineralization, providing that it occurred in the project areas.

The results of Area-A were shown in PL-67-69 in the Phase-I report, and those of Area-B were shown in PL-70-72, respectively.

As a result, very clear zonal arrangement was observed as described in 3-9-1: In Area-A, a zone of relatively high in copper is located near Cerro Bobí in the central part of the Area, whereas the zones of relatively high in Pb and Zn concentrically surround the former in the outer parts. The zones of relatively higher Zn to Pb are observed in two places; one is near Cerro Bobí overlapping the Cu-high, and another is near Pechác-Laurita at the northwestern corner of the area within the higher Pb and Zn to Cu.

In the proximity of Cerro Bobí, there occur small stocks of acidic intrusives of plutonic to hypabyssal nature. The zone of the Cu-high centers the stocks, and the zones of higher Pb and Zn surround the former.

These facts imply the genetical relationship between the mineralization and acidic intrusives, and further suggest that there might have occurred two types of mineralization, Cu-Zn, and Pb-Zn.

In Area-B, no obvious zonal arrangement is recognized as in Area-A, so far as geochemical assay values are concerned. However, a zone of relatively higher in Pb and Zn to Cu is present at the southeastern corner, and zones of both Pb/Cu and Zn/Pb highs that cross the area diagonally in NW-SE direction are clear distinguished.

These facts may suggest the existence of possible structural lines(3-9-1 of this report).

#### 4-4-5 Correlation analysis

In both Phase-I and -II, correlation coefficients between any two of the assayed elements were calculated by computer, together with other parameters. The results are summarized in Tables 10-A through D, and 12 in this report.

These results were utilized to infer the geochemical natures of populations in the two phases. The results of the Phase-II is summarized below.

High correlation was observed between any two of four elements Cu,Pb, Zn and Ag in Area A-1, and Area-C in the Phase-II. This implies that the most prominent mineralization within the present project areas may have been of a suit of Cu-Pb-Zn-Ag. On the other hand, tolerable correlation was observed only between Pb and Zn in Areas A-3, B-1, and B-3. This might offer two probable alternatives for these areas; one is that mineralization characterized by Pb-Zn occurred, another is that the anomalous values of Pb, and Zn might be attributed to abnormally high background of carbonate rocks rather than to mineralization.

#### 4-5 Selection and evaluation of target areas

##### 4-5-1 Selection of follow-up areas from Phase-I anomalies

Anomalies were delineated in a way described in previous 4-4-3. Major anomalies were then selected from them, based on their extents and assay values (Table-12). These areas were further compared with rolling mean highs, standard deviation highs, and geological maps, to study the inter-relation among them. Six relatively prospective areas were finally chosen around the major anomalies as the target areas of the follow-up operations in the Phase-II(total 297 sq.km).

Other than the aboves, an area (14 sq.km) surrounding the Llano del Coyote prospect was selected as a target of the Phase-II, through the studies on the existing information and data(p-43,44 in Phase-I report, and p-149,150 in Phase-II report). The prospect was first discovered by UN from geochemical anomalies of stream sediments. However, the area was not detected as geochemical anomalies in our 1st Phase operation, as little sample had been collected in the proximity of this area, to avoid duplication of works with UN. Nevertheless, in our rolling mean analysis,

the area is clearly expressed as highs of standard deviations. This substantiates the usefulness of the technique on localizing mineralized areas in the regional reconnaissance phase.

#### 4-5-2 Selection of target areas from Phase-II anomalies

Anomalies were delineated based on the same threshold values as in Phase-I, and eleven prominent ones were subsequently selected from them (Table-15, Fig. 4, 5, PL-5, 6). Four of them are located in Area-C Llano del Coyote to form practically a single anomaly. Therefore, it can be said in other words that eight anomalies were chosen.

These major anomalies were compared and studied on their extents, assay values, and geological factors. Furthermore, geochemical natures of the areas that include these anomalies were compared and examined from the patterns of the frequency distribution histograms and cumulative frequency curves, coefficient variances, and correlation coefficients of elements (P-53-60 in Phase-II report).

As a result, the following exploration priority was geochemically given to each of the anomaly and the area (p. 59, 60 in Phase-II report): "Taking an area as a unit, we consider conclusively that the Area-C ranks first, B-2 second, and A-1 third, from the viewpoint of the mineralization degree affecting that area. On the other hand, taking an actually localized anomaly as a unit, we may give following order; "No. 10 W18-E18 Anomaly in Area-C" ranks first, "No. 1 Peñasco-Pacumal Anomaly in Area-1" second, and "No. 2 East of Saclecán in Area A-2" and "No. 4 South of Estancia in Area B-2" third. For other areas and anomalies, it is fairly difficult to give ranks. For Area B-3, it may be necessary to re-check if there are any floats or outcrops of carbonates or sulfates of lead and zinc or not". These anomalies are summarized in Table-15 in this report.

Area-C Llano del Coyote was finally decided as the target area in the Phase-III. On determining the area, various factors other than the geochemical ones were also taken into account; those are geological occurrence of expected ore bodies, topography, location, limitation imposed on exploration term and budget, and so forth.



#### 4-5-3 Correlation between geochemical anomalies and drill result

Geochemical anomalies of soil samples, which were collected in Phase-II do not correlate very well to drill results (Fig.23); two of the tree DDHs that intersected "Zn-order Zn-mineralization" of sulfides (MJ-9, UR-4) are situated outside the anomalies of soil. This may be attributed to the facts: (1) In soil, indicators were dislocated to topographically lower position by supergene alteration and transportation of soil, so that the anomalies do not indicate exactly the position of the primary-dispersion halo on the surface. (2) The horizon of the major Zn-intersections rarely exposes on the surface.

On the other hand, geochemical anomalies of rock-chip samples that were collected on the surface in Phase-III, well correlate to drill results, exactly indicating the position of primary halos on the surface (3-8-1). These are discussed in more detail in 6-1 of Phase-III Report (PL-10 of Phase-III Rept.)

#### 4-5-4 On unexplored geochemical anomalies

Our present evaluation on the exploration potential of the unexplored areas, where no drill was performed in the present program, is not very different from what was described in the Phase-II report (p.59,60), which is also cited in the previous 4-5-2 in this report. However, a slightly positive factor may have been added to Area B-2, as promising Zn-mineralization was intersected in Area-C Llano del Coyote where the geological setting is very similar to Area B-2. Nevertheless, the area could not be an immediate exploration target, because its geochemical anomalies are by far the inferior in both size and values, being compared with those in Area-C. Our present conclusion is that only anomalies that are worth further exploration more or less, are Penasco-Pacumal anomaly in Area A-1, and East of Saculecán in Area A-2.

#### 4-6 Discussion

Geochemical survey was the most useful exploration tool in the present project, throughout the stages from the reconnaissance to the scout drilling.

Followings are our findings, suggestion, and recommendation on the further application of the exploration geochemistry in Guatemala, especially to a project similar to ours.

#### 4-6-1 On indicators and path finders

Three elements Cu, Pb and Zn were adopted as indicators in the 1st phase program, and Ag was added to the three in the 2nd phase.

It is recommended to add at least Au for a further program in other areas, so far as the exploration for non-ferrous metals are concerned: Gold is useful as an indicator, not only for the gold exploration, but also for the basemetal exploration, especially in an area where the leached capping exist. For, gold tends to remain enriched in the leached capping, and often becomes a clue of the discovery of a base metal deposit, especially of copper.

Analytical method of gold for the purpose of the exploration geochemistry is somewhat troublesome, but recently, AAS technique with solvent extraction is frequently used for this purpose.

It is quite necessary to select carefully the most effective indicators and/or path finders in accordance with the objective metals and the geology of the target areas, when an exploration program is planned.

#### 4-6-2 On data processing method

Through the present project, it has been revealed that the rolling mean analysis is very much useful especially in the reconnaissance phase. Of the technique, the standard deviation highs well indicated the existence of the mineralized parts. Therefore, it is recommended to apply this technique in the reconnaissance stage of a further project similar to ours.

On the determination of the dimension of a search area in the analysis, it is suggested to study application of the variogram in the Krigging method (Krige; 1951, Matheron; 1963, 1971) to this purpose, as the search area in the present project was rather arbitrarily determined as 10-UTM grid-square without any theoretical support.

#### 4-6-3 On threshold values

It may be recommended to apply the rolling mean analysis technique to the determination of the threshold values: It may be more reasonable to define the threshold values as a surface of "mean + 2 standard deviations (calculated from all the samples falling in a search area)" in the rolling mean analysis. In this case, an area where the actual assay values of the samples are beyond the surface is to be defined as an anomaly or anomalous area.

"Lepeltier's method" cannot always be appropriate as a technique to determine the threshold values, as it is often rather subjective due to numerous breaking points on regression lines. However, it is quite useful as a mean to know the nature of a population.

Therefore it is worth practicing the technique, no matter whether it is used as threshold or not.

#### 4-6-4 Limonite zone and geochemical results

In general, interpretation of geochemical data is complicated in a place where pervasive and intensive limonitization occur on the surface as in the case of Llano del Coyote. Because, copper tends to form a leached capping in such a place, while lead and zinc tend to form secondary enrichment in the oxide zone.

It has been revealed from the correlation among drill results, and geochemical anomalies of soil and rock-chip samples that geochemical and geological environments in Llano del Coyote prospect are much more complicated than the above: (1) The skarn horizon of major Zn-mineralization rarely exposes on the surface, so that anomalies which may be reflected on the surface in this area are to be primary-dispersion halos, (2) in soil samples, indicators were displaced by secondary dispersion to topographically lower positions, so that soil anomalies do not indicate exactly the positions of primary-dispersion halos on the surface, (3) Zn contents in rock-chip samples seemingly became more enriched than in original rocks, so that they became easier to be detected, (4) the presence of secondary enrichment of copper was confirmed by DDHs here and there underneath the geochemical anomalies of rock-chip samples.

As mentioned above, it is impossible to establish standard criteria to evaluate geochemical data in the limonitized zone. However, it is necessary and worth to explore the primary and/or secondary sulfide zone

by drills, if copper or Zn values of say  $n \times 10^2$  ppm or more are widely detected in soil samples in such an area where the leached capping is anticipated from the geological observation. It may be recommended to carry on rock-chip sampling before to decide drill locations, in order to locate more exactly either the intersection of ore and the surface, or that of primary-dispersion halos.

#### 4-6-5 Pb-Zn anomaly in carbonate rocks

In the terrain of carbonate rocks, Pb and Zn often tend to concentrate near the surface to show abnormally high background in soil samples. The huge "anomaly" in Area B-3 might be attributed to such cause. Therefore, it is particularly required to distinguish the "anomaly by mineralization" from the "apparent anomaly".

Followings are our findings on the difference in geochemical characteristics between the anomalies that were obviously attributed to mineralization and those of ambiguous nature: (1) Fairly strong correlation was observed among Cu, Pb and Zn in the anomalies, in which known mineral showings are present (A-1 and A-2). On the other hand, little correlation was recognized in Cu-Pb and Cu-Zn in Areas B-1 and B-3, where either showings or ore floats were rarely observed. (2) Standard deviation highs in the rolling mean analysis well coincided with the areas where known mineralization occurs.

These may provide clues to distinguish the two, though it can not positively be asserted as yet.

#### 4-6-6 Geochemical exploration by rock-chip samples

Geochemical exploration by rock-chip samples was carried out in Phase-III. As a result, it has been revealed that anomalies of rock-chip samples well reflect halos by primary-dispersion of mineralization, and very well correlate to drill results (6-1-2 in Phase-III Rept.): All the three DDRs that intersected "%-order Zn-mineralization" are located in the Zn-anomalies delineated by 500 ppm, and the presence of the "secondary enrichment" of Cu with supergene chalcocite was confirmed in several DDRs that are located in the Cu-anomalies delineated by 500 ppm.

On this subject, description and discussion are made in 6-1 in Phase-III Report.

## 5 Geophysical Survey

### 5-1 Introduction

Geophysical survey was carried out in the 2nd phase of the present program in Area-C Llano del Coyote, simultaneously with geological mapping, geochemical sampling, and pilot DDHs. The survey comprised IP (induced polarization) and ground magnetic survey. Here, only a brief review of the survey is made, as the detail is described in Part-III of the Phase-II report.

The present project area (7km x 2km = 14 sq.km) includes an area where UN undertook an exploration program in 1969 and 1979; they also carried out geological mapping, geochemical sampling, EM, IP, ground magnetic survey, and 7 short DDHs to IP anomalies (UN;1973, and p.149 in Phase-II report).

The reason why we intended to re-explore the area is mentioned in I-1 in this report, and p.149 to 150 in Phase-II report.

The reason why we selected IP as an exploration technique in the 2nd phase is as follows: (1) The IP located by UN are still open to both NW and SE. (2) It was required to reveal the distribution of sulfides below the oxide zone, as little sulfides are observed both on the surface and in the UN drill cores down to 30 to 70m from the surface, though the surface is covered widely by the limonitized outcrops and floats (the existence of the leached capping was anticipated). (3) Few UN DDHs reached the expected depth of their IP anomalies, though the drills had been planned to explore them. (4) It was anticipated through the review of UN data that there might be a mineral zoning in a manner of Cu-Pb & Zn-IP anomaly (pyrite). Therefore, IP was considered to be helpful for the interpretation of the geochemical anomalies, even if it only indicated pyritization in the bed rocks.

The reason why we selected the ground magnetic survey is because the floats and outcrops of massive magnetite intermittently but widely occur on the surface area.

Some DDHs were carried out in the Phase-III to explore these IP anomalies, but they only resulted in to reveal that the IP anomalies were caused by strong pyritization: Most of DDHs laid in IP anomalies intersected strong pyritization, which is locally concentrated up to semi-massive

to massive pyrite (S=15 to 20% for several m). However, all the three DDHs that intersected "%-order Zn-mineralization" are located outside, or at the margin of IP anomalies (Fig.23).

No conclusion can be made on applicability of magnetic survey, as no drill has been done in the most prominent inferred magnetic body between W4 and O-lines. This anomaly may be attributed to magnetite concentration in depths, as gossan with hematite occur scatteredly on the surface of this area. A widely distributed but weak inferred magnetic body, which coincides approximately with IP anomalies and includes the prominent inferred body mentioned above, may be derived from magnetite in the pyrite zone. The magnetite occurs pervasively and may reach several % in average, though no exact data for evaluating its average content is available as yet.

The correlation among geophysical anomalies, geochemical anomalies by soil samples, geological background, and drill results is summarized in Table-16, and spatial relationship among them is illustrated in Fig.23 of this report. The relationships among drill results, geochemical anomalies by rock-chip samples, and geology are shown by far the better in PL-5 and Fig.10 in Phase-III Report.

#### 5-2 Works carried out

The geophysical survey was carried out in the following terms in 1977: Chaining of the base-lines and picket-lines; from September 20 to October 15. The field IP measurements; from October 2 to 18. The ground magnetic survey; from October 9 to 25.

The summary of the works carried out is as follows.

|                              | Induced polarization<br>(Frequency domain) | Ground magnetic<br>Survey |
|------------------------------|--|---------------------------|
| Covered area                 | 13.6 sq.km                                 | 14.0 sq.km                |
| Total length of picket lines | 42.0 line.km                               | 72.0 line.km              |
| Number of picket lines       | 21   | 36                        |
| Length of a picket line      | 2.0 km                                     | 2.0 km                    |
| Picket line interval         | 400m(200m)                                 | 200m                      |
| Station interval             | 100m                                       | 100m                      |

### 5-3 Induced polarization(IP)

#### 5-3-1 Kinds of works and their specifications

Field IP measurements were carried out by two field parties with frequency domain system technique. The two parties used equipments of different brands, so that different ranges of the frequencies were used. These are as follows: A-party used  $AC_L=0.3$  Hz and  $AC_H=2.5$  Hz, whereas B-party used  $AC_L=0.3$  Hz and  $AC_H=3.0$  Hz. Dipole-dipole configuration was adopted for earthing(Fig.22). Separation factor of electrode was varied from 1 to 4 in usual measurement, while it was increased to 5, where strong frequency effect(FE) was detected. The general explanation on the principle and the application methods are briefly described in p.187 of the Phase-II report.

Laboratory IP measurements on handspecimens were practiced in Japan, in order to provide the basic data for simulation analysis and to facilitate the interpretation of the IP results obtained from the field measurement. Frequency effect(FE) and apparent resistivity(AR) were measured on 38 handspecimens collected from the surface of the project area. Details are described in p.192-202 in the Phase-II report.

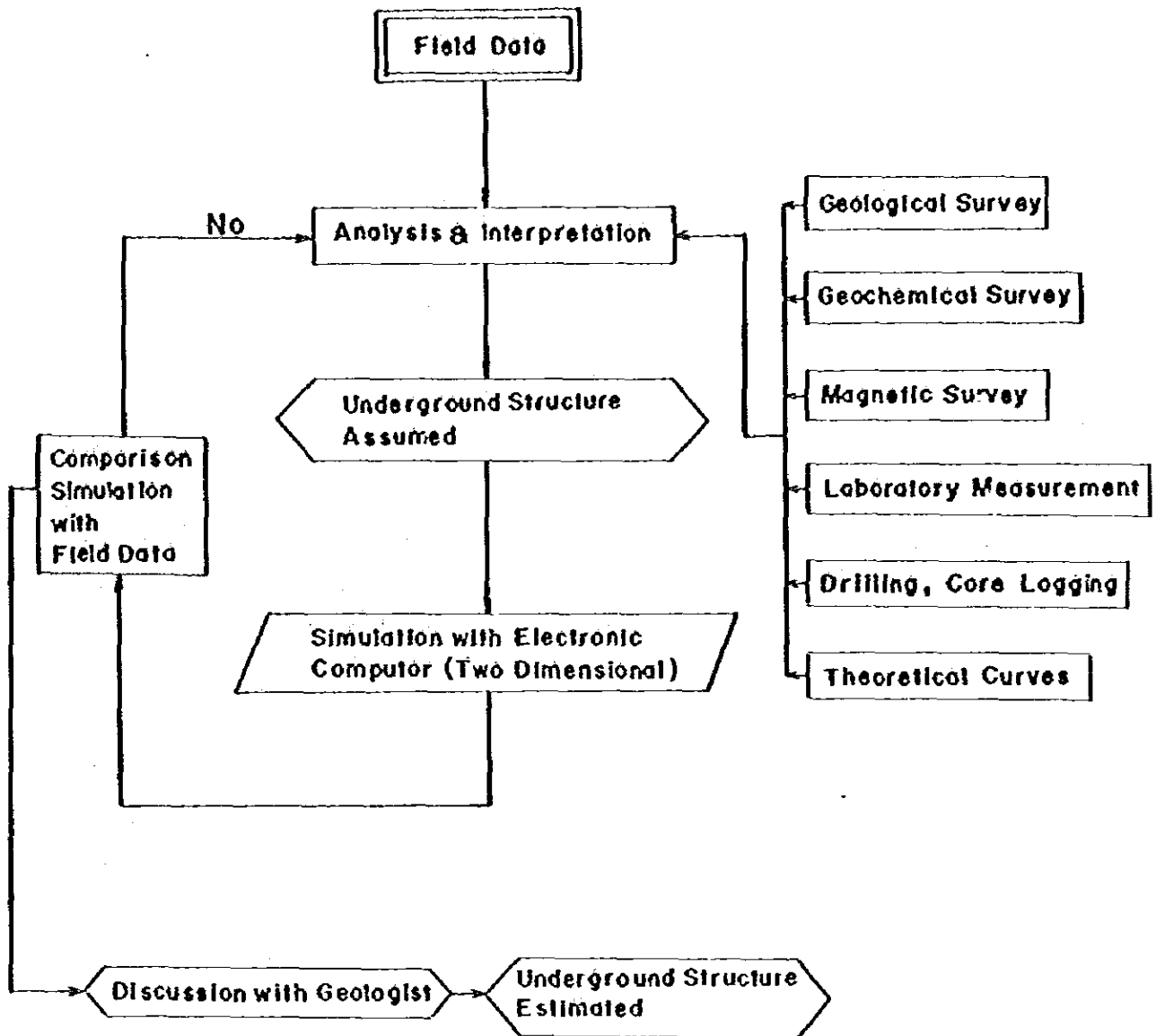
Two dimensional simulation analysis was carried out on selected 4 profiles along picket lines. The lines selected are W6, O,E4, and E12, all of which are located in the central zone of the inferred mineralization (Fig.23). The data which were utilized for the simulation are the results of the field IP measurements, the laboratory IP measurements and the ground magnetic survey, and geological informations. On simulation, both analogue computer and digital electronic computer were utilized. The details of the simulation analysis are described in p.202-208 in the Phase-II report, and the procedure of the simulation analysis is illustrated in a flow chart(Fig.21)

#### 5-3-2 Field measurements and equipments



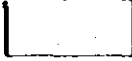
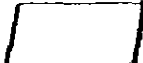
The field measurements were performed by two field parties, A and B. The-A party covered an area from the line-W2 westward, while the B-party covered an area from line-O eastward, respectively.

The equipments used by the two parties are summarized below, as well as the frequency ranges. More detailed information on equipments is given in p.191 of the Phase-II report.

Fig. 21 Flow Chart of Simulation



Index

-  Measurement
-  Estimation
-  Analysis, Interpretation, Mapping
-  Calculation



|                         | A-party        | B-party                                 |
|-------------------------|----------------|---|
| Frequencies used: $C_L$ | 0,3 Hz         | 0,3Hz                                   |
| $C_H$                   | 2,5Hz          | 3,0Hz                                   |
| Transmitter             | McPhar P-660TX | Chiba Electronic Laboratory CH-505A,B   |
| Receiver                | McPhar P-660RX | Yokohama Electronic Laboratory YDC-434B |
| Generator               | McPhar 70223   | McCulloch Mark-II 400                   |
| Checker                 | -              | Yokohama Electronic Laboratory YN-502   |

As the two parties had to use different frequencies for  $C_L$ , a trial measurement was practiced for correlation purpose, prior to the main field operation. The measurement was made by each party at the same stations on the same line(Line-0). However, as a result, it was decided to use the measured values by two parties without any correction and/or standardization, as it was judged there were no practical difference between two sets of measured values (p.191-192, and Table GP-2 in the Phase-II report).

### 5-3-3 Results and their presentation

Frequency effect(FE) was directly measured, and apparent resistivity (AR) was subsequently calculated from the electrical current and potential difference. Metal conduction factor (MCF) was obtained from the frequency effect and the apparent resistivity. The definitions of these three parameters, FE,AR, and MCF are as follows.

#### Apparent Resistivity (AR)

An apparent resistivity in Dipole-Dipole configuration of electrodes is calculated by the following formulas.

$$AR = \rho_a = K \cdot \frac{V}{I} \quad (\Omega\text{-m})$$

where:  $K = a \cdot n \cdot n(n+1)(n+2)$

$\rho_a$  = apparent resistivity ( $\Omega\text{-m}$ )

K = geometrical factor

V = difference in potential (mV)

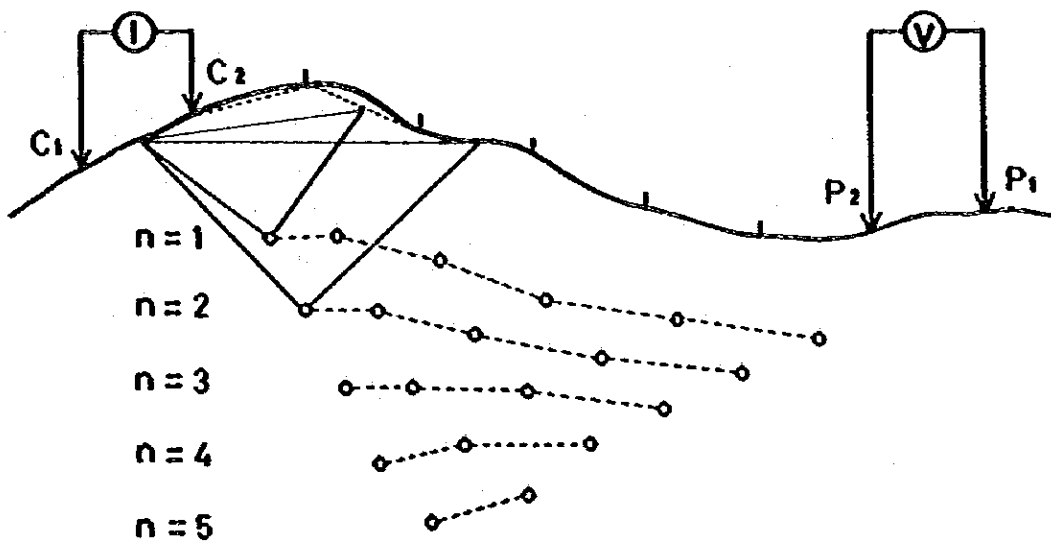
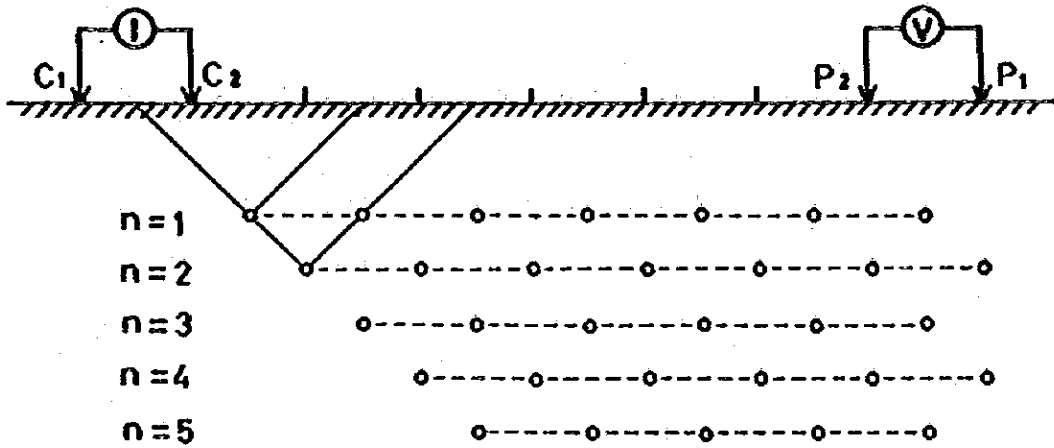
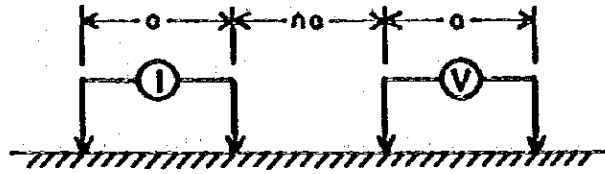
I = electrical current(mA)

a = space of electrodes

n = separation factor of electrodes

Fig. 22

Dipole - Dipole Configuration



### Frequency Effect (FE)

In the frequency domain system, apparent resistivities by two kinds of frequency are measured, and IP effect is obtained by normalizing the difference of two apparent resistivities, which is commonly called "Frequency Effect-FE". FE is defined as the following formula.

$$\begin{aligned} FE &= \frac{V_L - V_H}{V_H} \times 100\% \\ &= \frac{\rho_{aL} - \rho_{aH}}{\rho_{aH}} \times 100\% \end{aligned}$$

where: FE= frequency effect (%)

$V_L$  = difference in potential by low frequency (mV)

$V_H$  = difference in potential by high frequency (mV)

$\rho_{aL}$  = apparent resistivity by low frequency ( $\Omega\text{-m}$ )

$\rho_{aH}$  = apparent resistivity by high frequency ( $\Omega\text{-m}$ )

### Metal Conduction Factor (MCF)

As many of metallic sulphides have lower resistivity and higher FE, the ratio of FE to apparent resistivity is used in order to express the effect of metallic minerals. This is called "Metal Conduction Factor-MCF", and it is defined as

$$MCF = \frac{FE}{\rho_{aH}} \times 1000 \text{ mho/m}$$

The values of AR, FE, and MCF were plotted in each section along the picket line in a way as follows: a value is plotted at the apex of right-angled equilateral triangle whose base is a linear segment connecting the center points of both the current electrodes (C1, C2) and the potential electrodes (P1, P2) (Fig. 22). Contours were drawn, and were transferred to level plans corresponding to separation factors (PL-79 to 90 inclusive), attached to the Phase-II report.

#### 5-3-4 Summary of the results

The results are described in detail in p.208-217 in the Phase-II report, and are presented in maps, attached to the same report (PL-79 through 96 inclusive). Therefore, only very brief description is made here. The anomalies of AR, FE, and MCF on a level about 150m below the surface (n=3) are composited in Fig.23 of this report, as well as major magnetic and geochemical anomalies, and drill locations.

##### (A) Frequency effect

The FE values within the investigated area range from 0.2 to 6.8%, though most of them are less than 2.0%. On the other hand, the values exceeding 3% are geographically concentrated in some particular areas. From these geographical and frequency distributions, the anomalous values in FE in the area were decided as those which exceeded 3%.

FE anomalies are mostly located in the central part of the area, between W24 and E24, and extend in the WNW-ENE direction for over 4.8m nearly parallel to the base-line. The anomalies were further divided into three groups, based on the geographical distribution. These are; (1) anomaly centered on line-W24, (2) anomalies that extend in the EW direction between W16 and E16, (3) anomaly centered on line-E24.

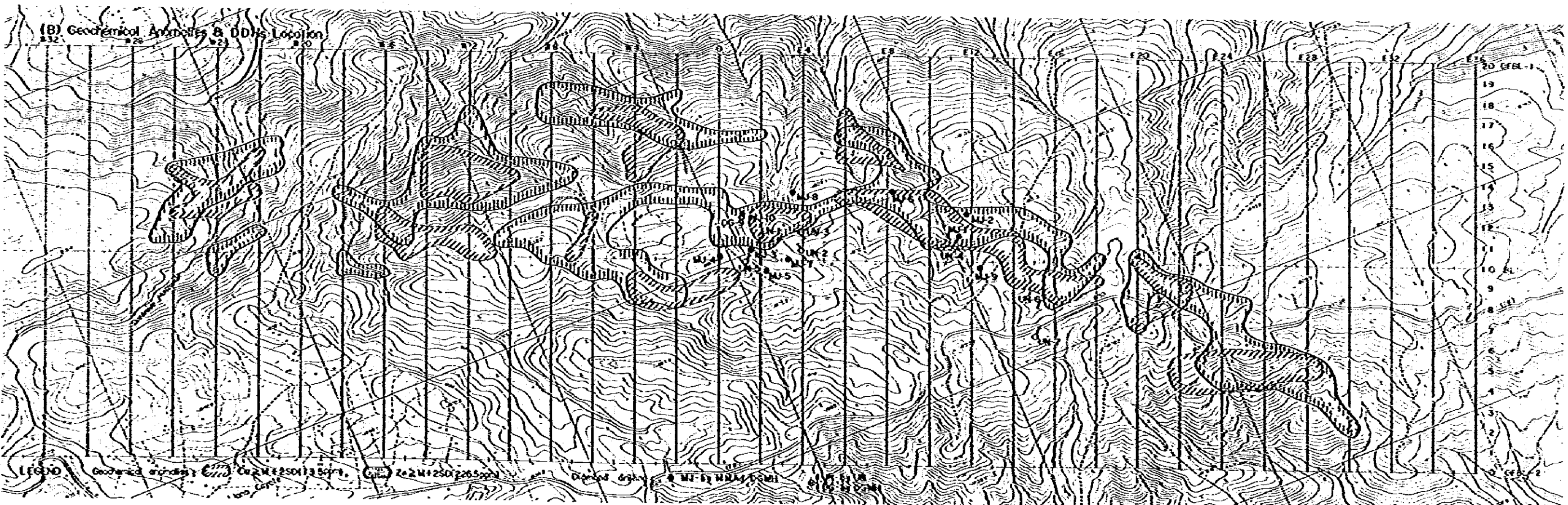
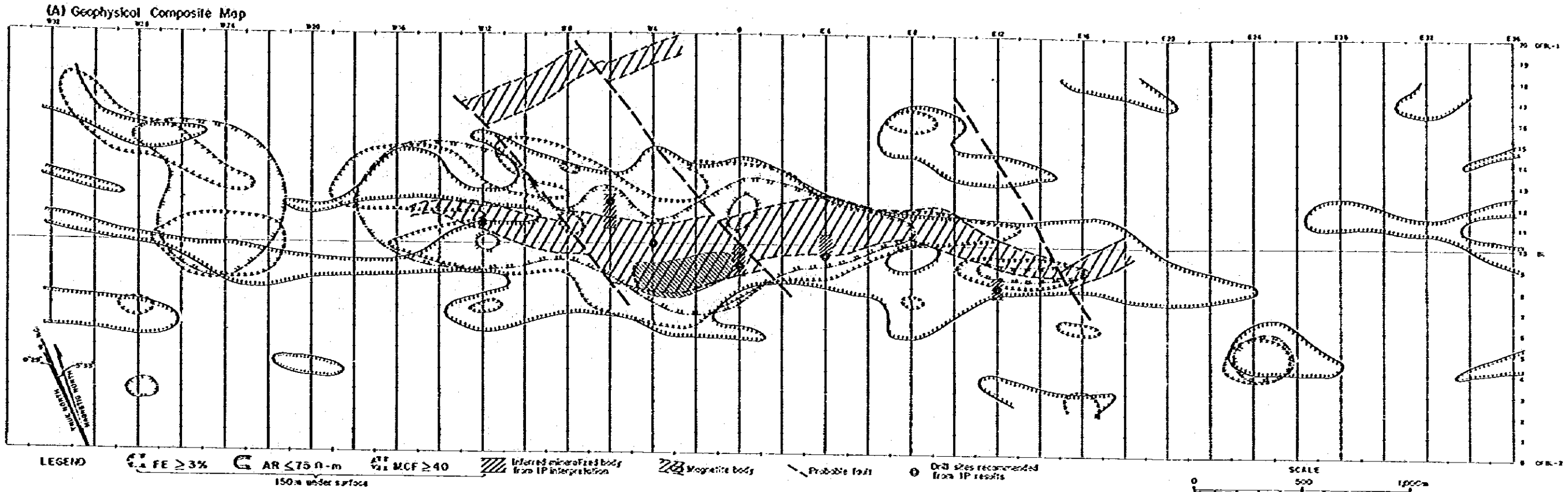
##### (B) Apparent resistivity

The AR values in the area range from 10 to 1,084  $\Omega$ -m. However, the values less than 200  $\Omega$ -m occupy more than 90% of the total areas in areal distribution, and the ones more than 200  $\Omega$ -m are only in the extremely limited areas. Of these, the values less than 75  $\Omega$ -m show comparatively concentrated pattern in areal distribution. Based on these observations, the investigated area was divided into three groups; (1) low AR zone with the values lower than 75  $\Omega$ -m, (2) intermediate AR zone, with the values between 75 and 200  $\Omega$ -m, and (3) high AR zone with the values higher than 200  $\Omega$ -m.

All these zones occur elongated in the E-W direction. The intermediate zone was considered to represent the background of the area, from its wide distribution both in area and in frequency.

The low AR zone occurs in the central area along the base-line. It comprises an aggregate of smaller anomalies at the shallower depth, whereas it becomes more simplified in form, on going deeper. This may be interpreted that at a shallower depth a measured AR value stands for only the

Fig.23 Geophysical- Geochemical Anomalies & DDHs Location



| $\rho(\Omega\text{-m})$ | FE (%) |
|-------------------------|--------|
| 1 100                   | 2      |
| 2 50                    | 2      |
| 3 10                    | 20     |
| 4 500                   | 2      |

values of rocks within a limited small area, while it becomes much affected by rocks of much wider surrounding areas so that its local characteristic becomes diluted.

The high AR zone mostly occurs in both southern and northern parts of the low AR zone. However, the areas of individual anomalies are so small that few anomalies occur straddling two adjacent picket lines.

The geographical distribution of the low AR zone well coincides with the anomalies of the FE. Especially on the level  $n=4$  between W-16 and E-16, the two are quite the same both in pattern and in elongation.

### (C) Metal conduction factor

The MCF values in the area range from 1 to 354 mho/m. The anomalous values are to correspond to those more than 40 mho/m from the definition of MCF, because the FE anomaly was defined as over 3%, and the low AR anomaly as lower than 75 ohm-m.

The MCF anomalies well coincide with those of the FE as a whole, especially in an area between W16 and E16, where the major anomalies of the MCF occur. This is quite natural, as the FE anomalies and the low AR anomalies occur overlapped each other in this part.

However, two fractional MCF anomalies that occur around W28 and W28 are the ones due to extremely low AR values, rather than high FE.

### (D) Simulation analysis

As the result of the simulation analysis, it was inferred that the anticipated mineralized bodies (ore body model) might show vein-like structures dipping vertical or steeply to the south. It was also inferred that the ore body model, as a whole, might plunge to the east, as its top level seemed to be shallower in the western sections W2 and, 0 while to become deeper in the eastern sections E4 and E12.

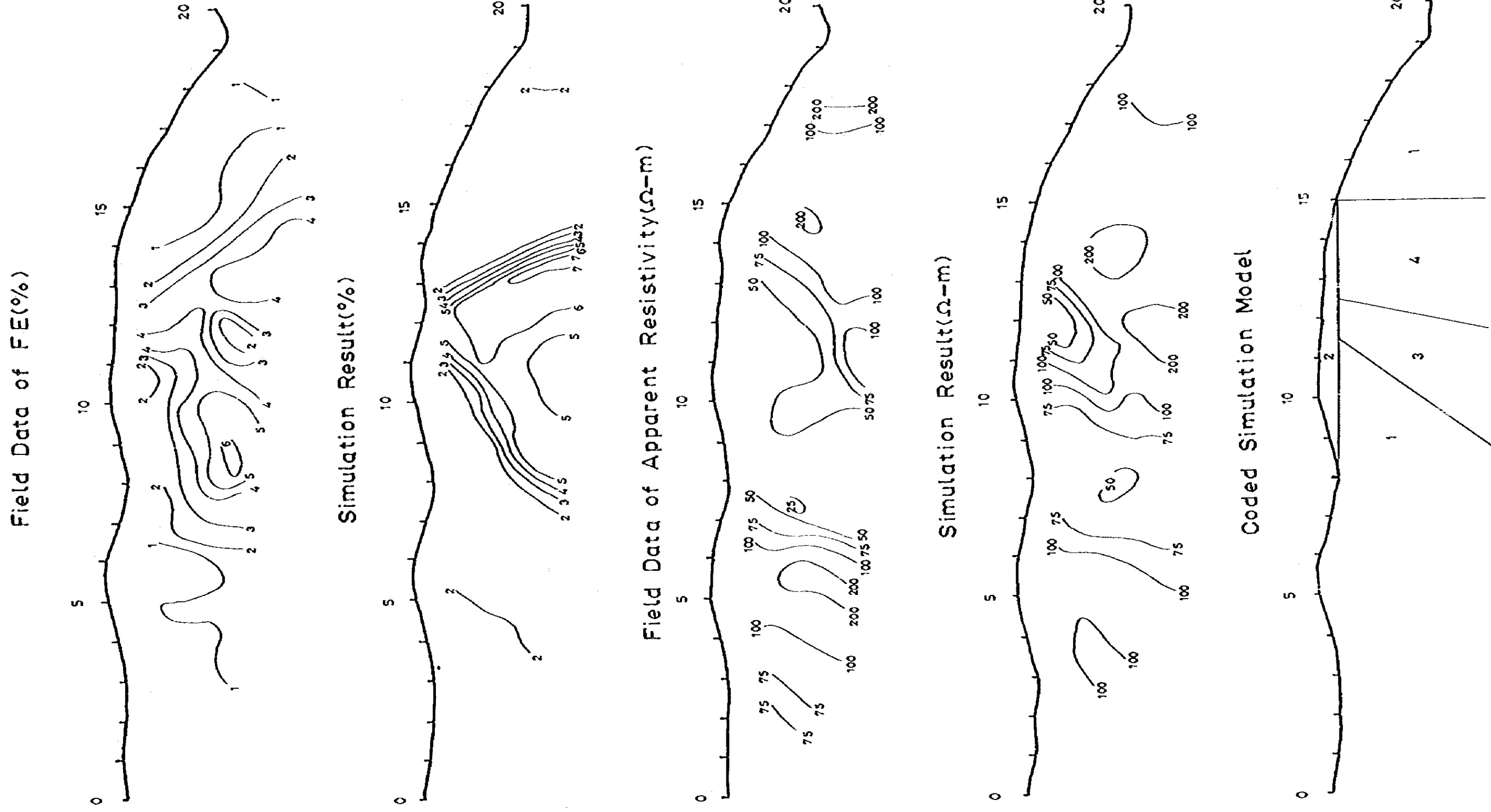
Summary of the findings on each lines are described below.

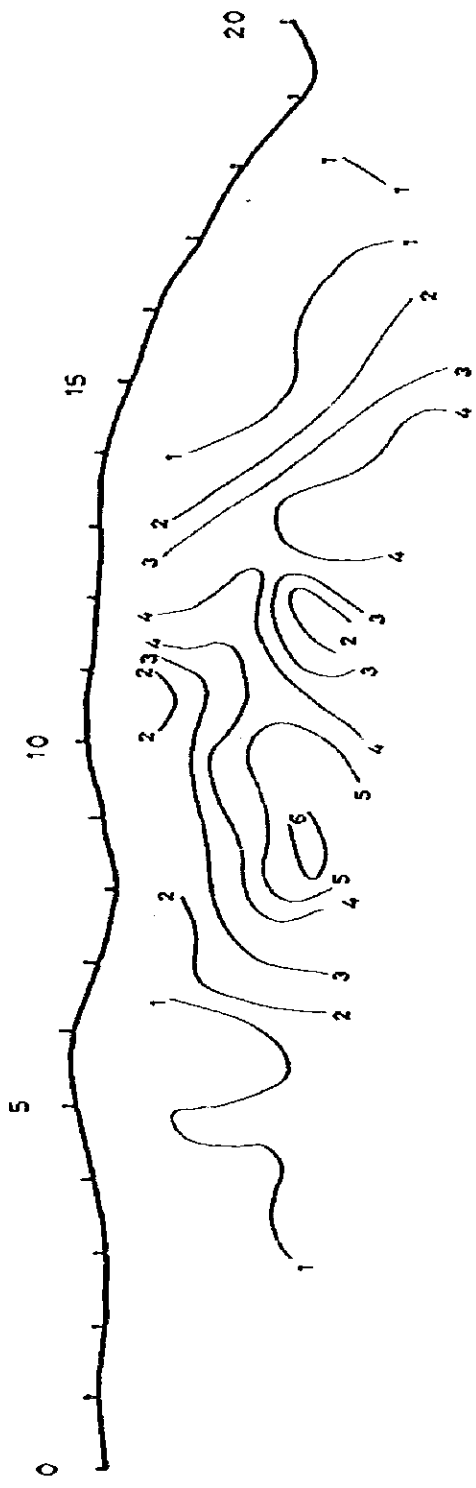
**Line-W6 (Fig.24):** The ore body model is southward dipping, top of which is centered in the vicinity of station 12 and the thickness of which increases in proportion to the depth, having FE of 20% and resistivity of  $100\Omega\text{-m}$ . The top of the model is approximately 50m below the ground surface with an overlying low-AR layer ( $50\Omega\text{-m}$ ) of 2%, FE between it and the surface. A  $100\Omega\text{-m}$  AR layer of 2% FE is distributed on the south side and a  $500\Omega\text{-m}$  high AR layer of 2% FE on the north side in this structural model. Farther to the north of the high AR layer, a layer with similar properties to that on the south side is assumed to exist.

Fig-24

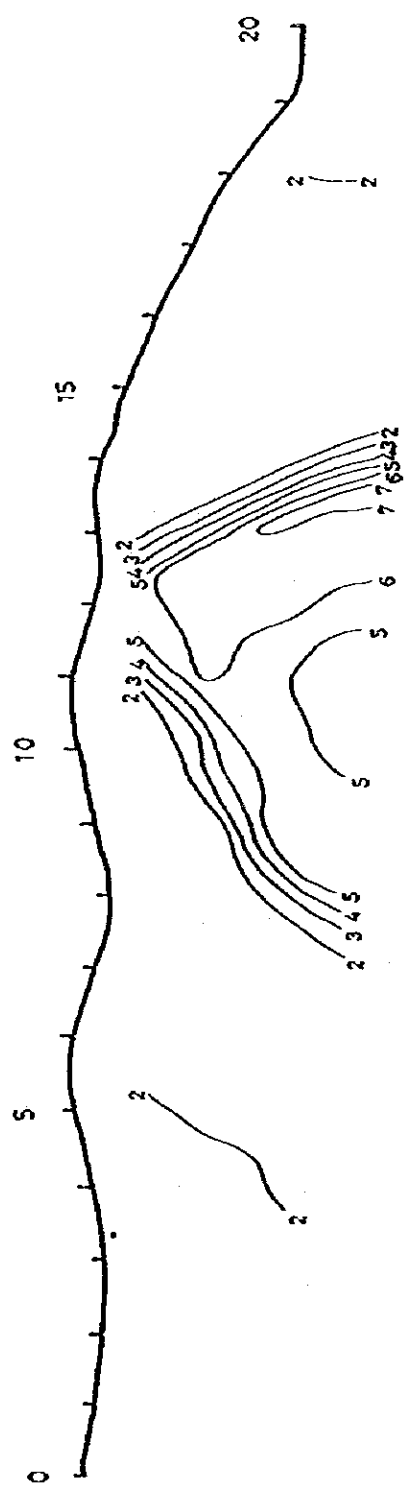
Results of Simulation Analysis for Line-W6

Scale 1:10000

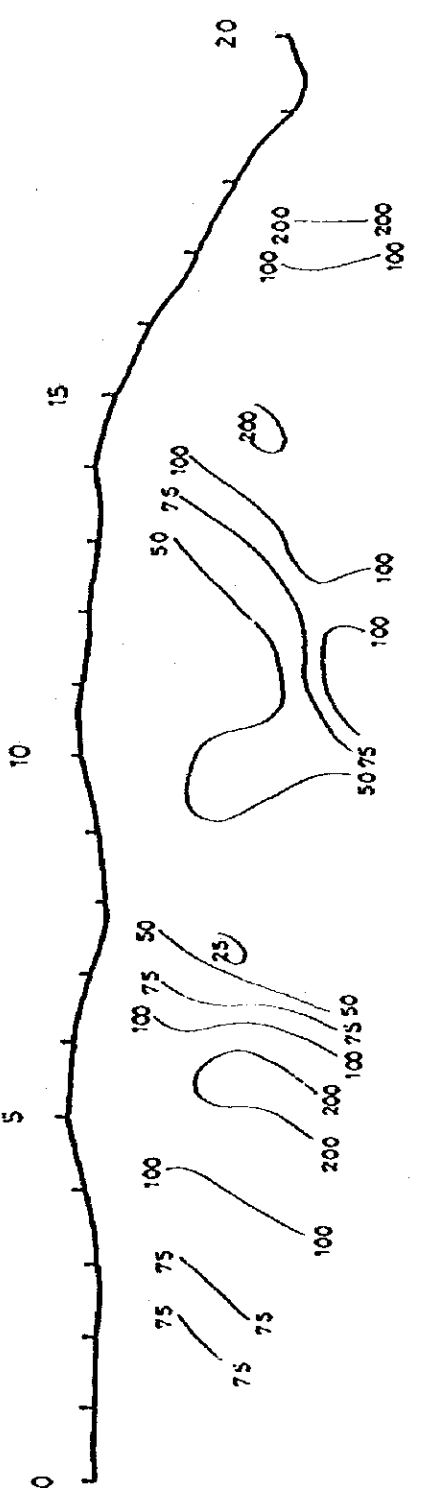




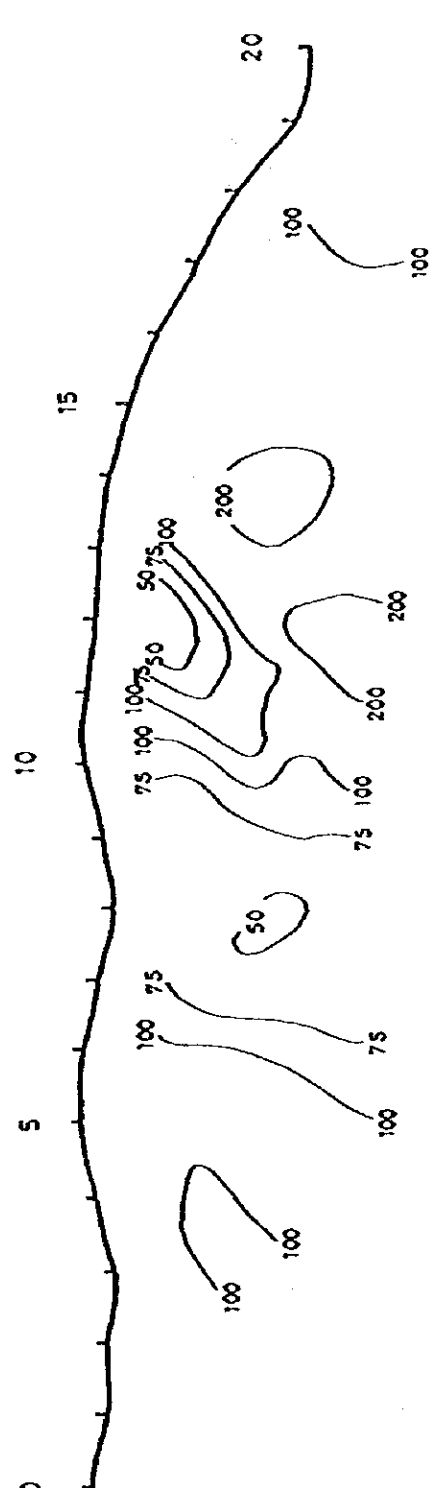
Simulation Result(%)



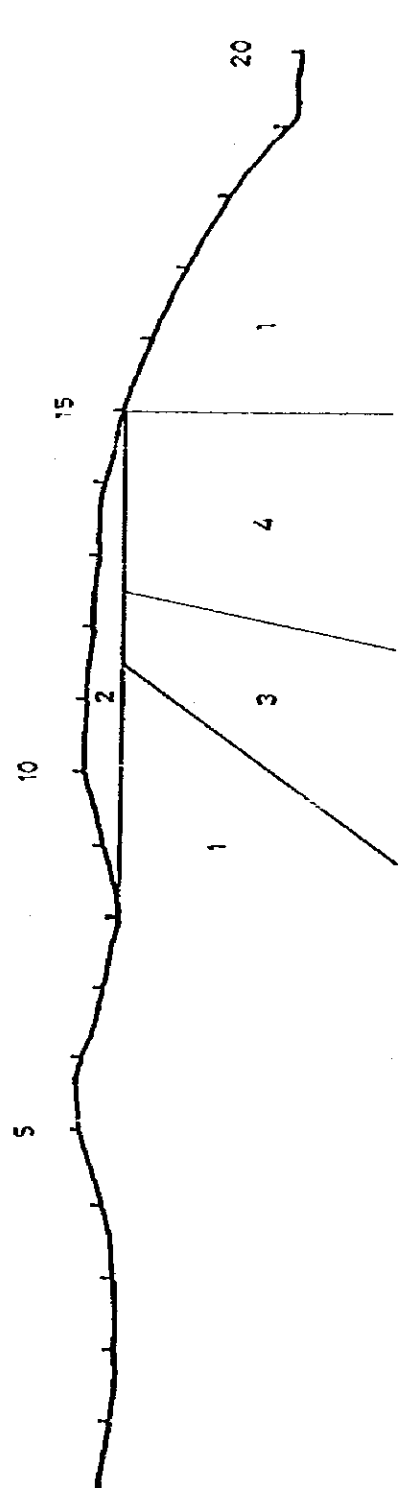
Field Data of Apparent Resistivity( $\Omega$ -m)



Simulation Result( $\Omega$ -m)



Coded Simulation Model



|   | $\rho(\Omega\text{-m})$ | FE(%) |
|---|-------------------------|-------|
| 1 | 100                     | 2     |
| 2 | 50                      | 2     |
| 3 | 10                      | 20    |
| 4 | 500                     | 2     |

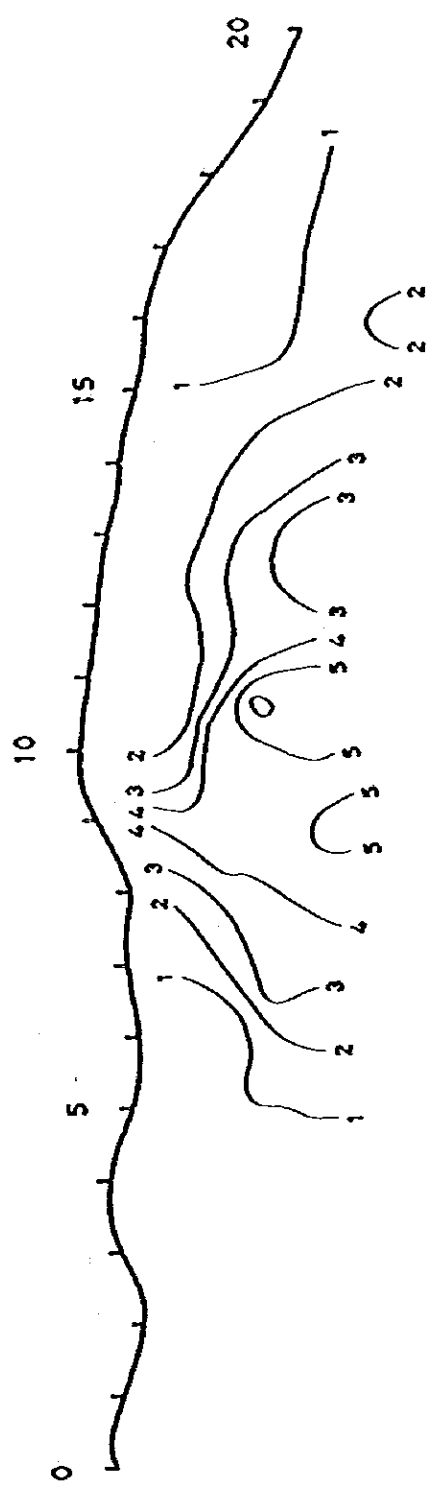


Fig. 25

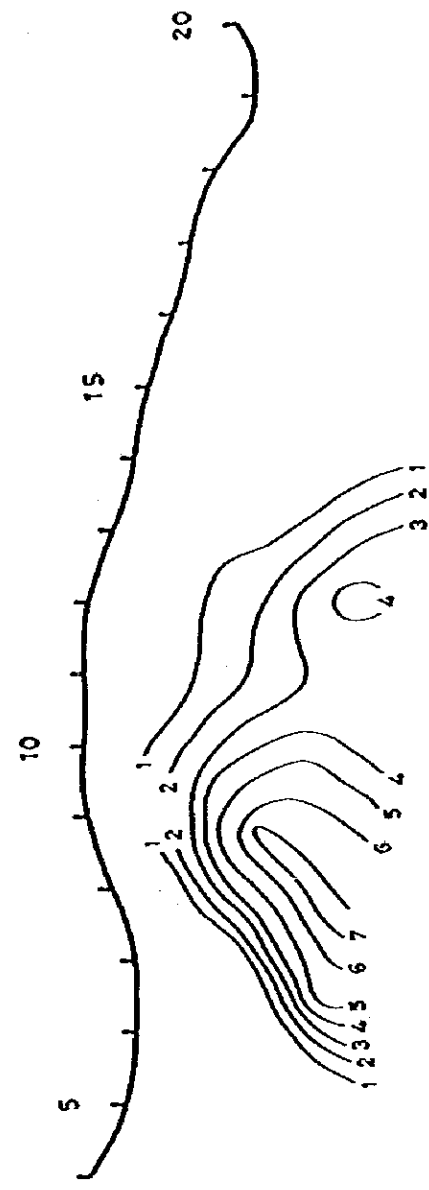
Results of Simulation Analysis for Line-0

Scale 1:10000

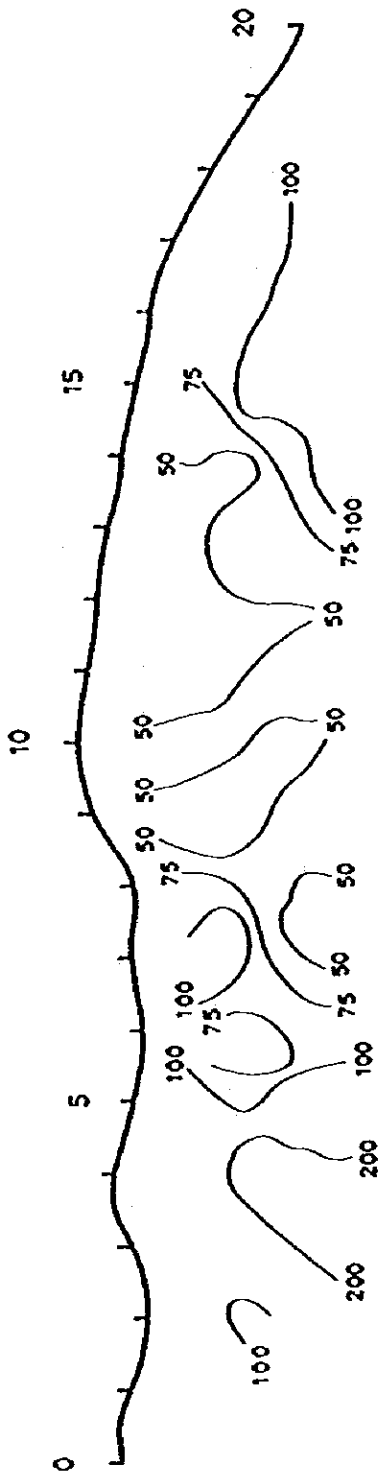
Field Data of FE(%)



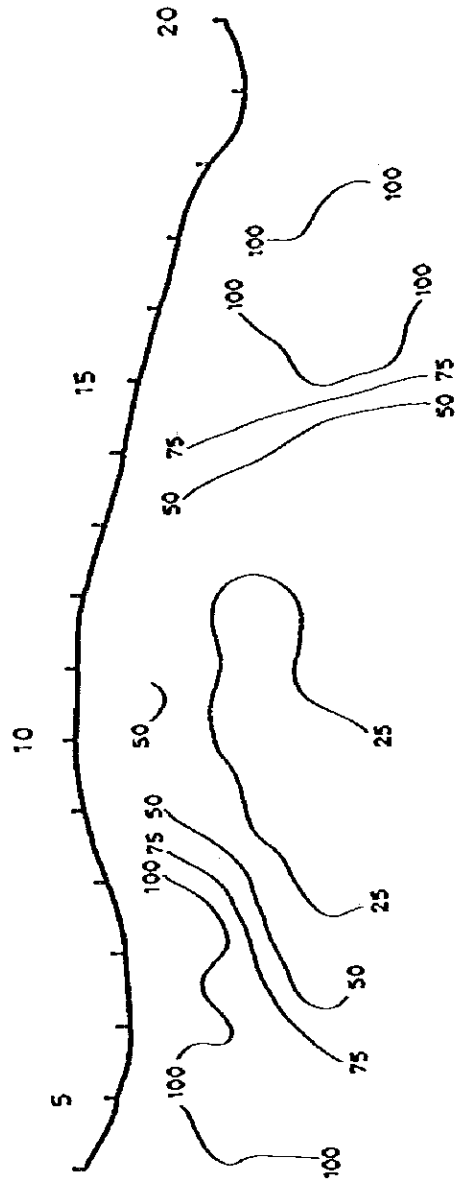
Simulation Result(%)



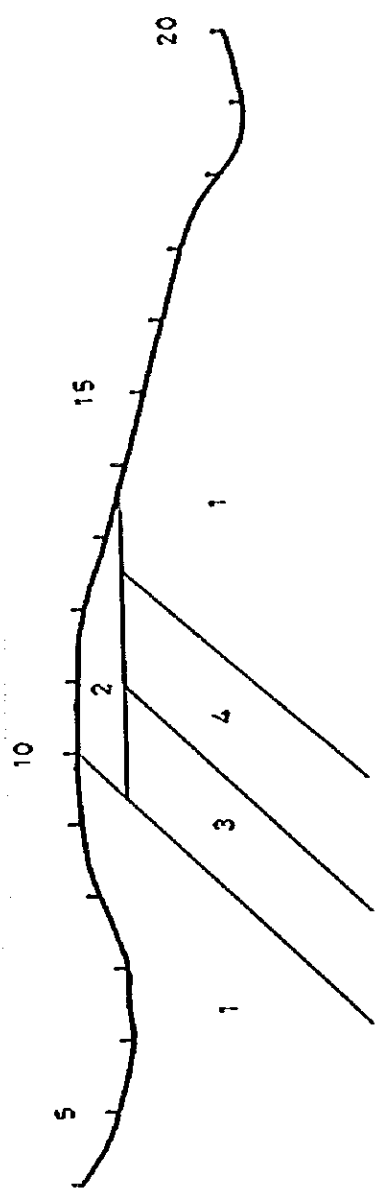
Field Data of Apparent Resistivity( $\Omega$ -m)



Simulation Result( $\Omega$ -m)

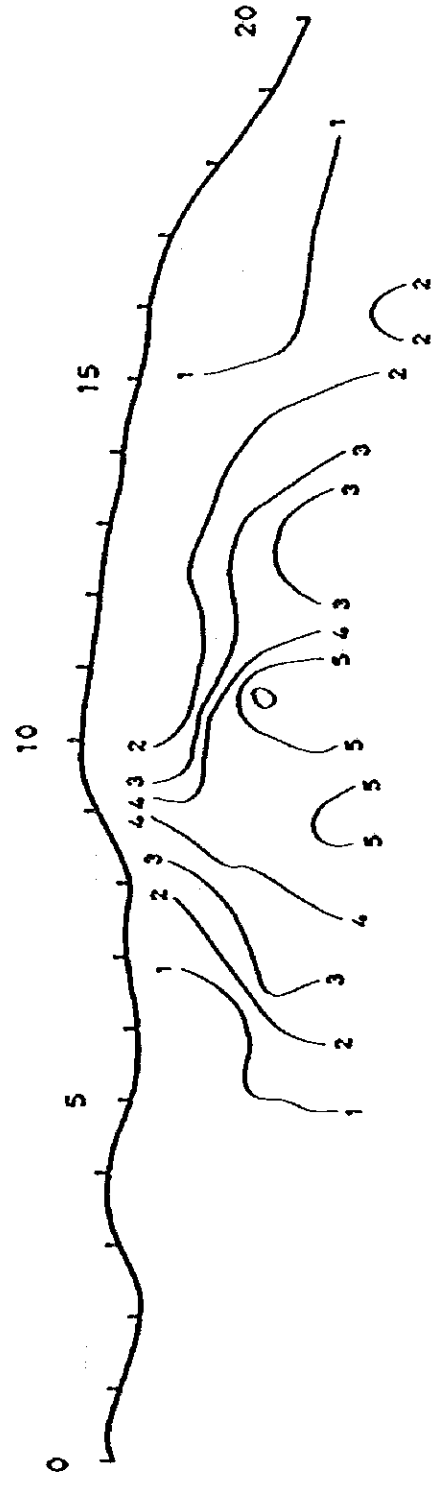


Coded Simulation Model

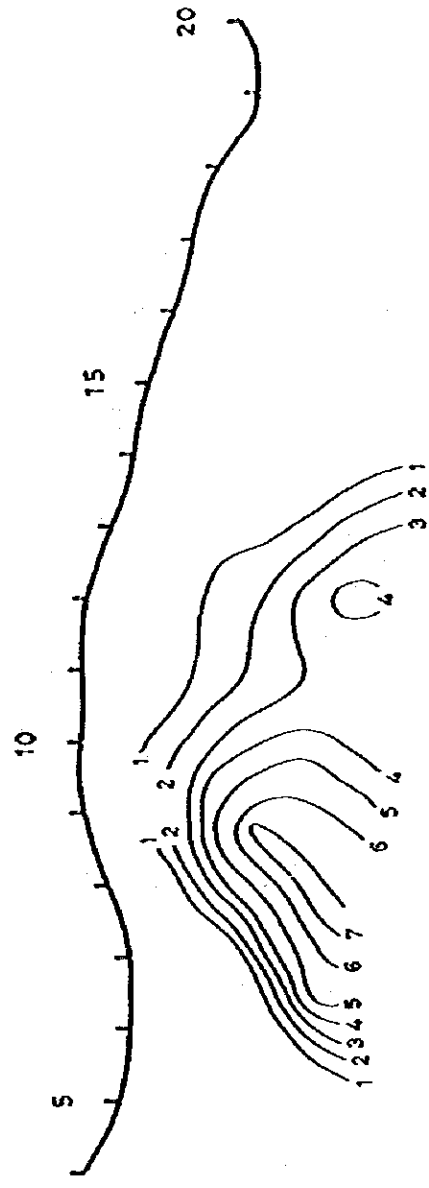


| $\rho$ ( $\Omega$ -m) | FE(%) |
|-----------------------|-------|
| 1 100                 | 2     |
| 2 50                  | 2     |
| 3 10                  | 15    |
| 4 10                  | 2     |

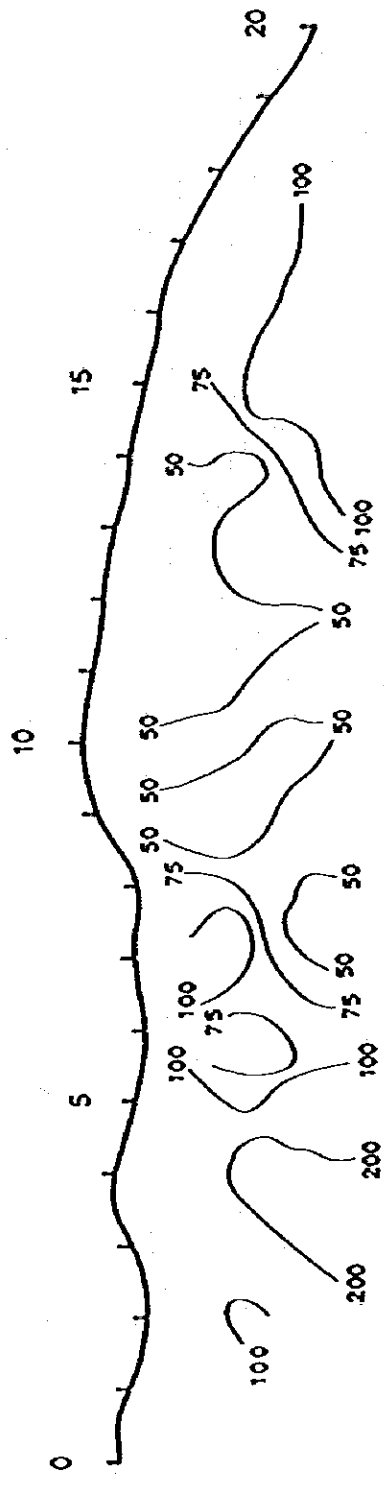
Field Data of FE(%)



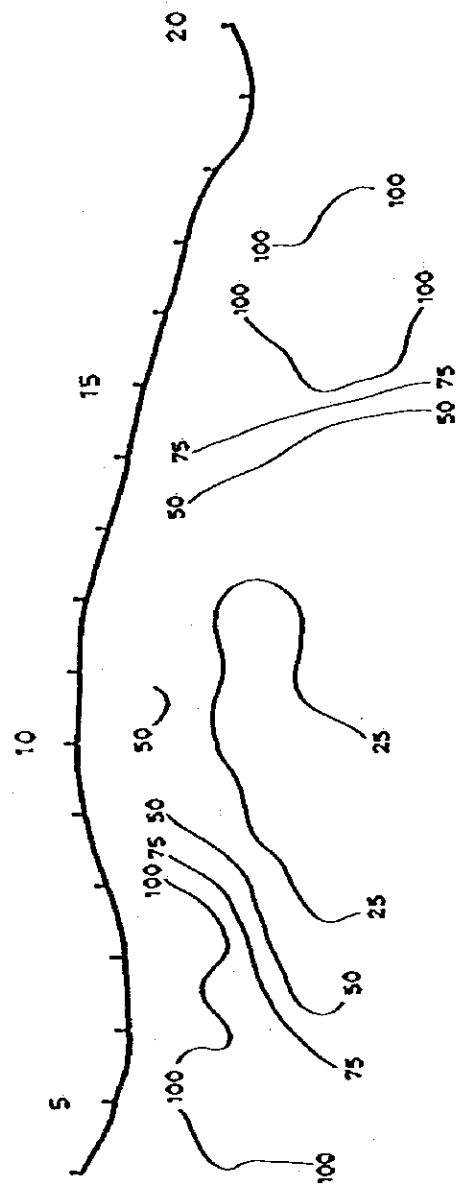
Simulation Result(%)



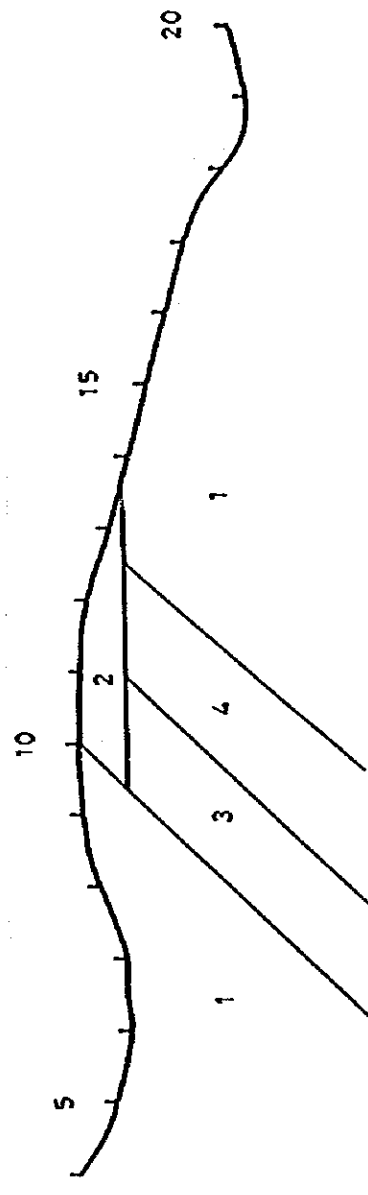
Field Data of Apparent Resistivity( $\Omega$ -m)



Simulation Result( $\Omega$ -m)



Coded Simulation Model

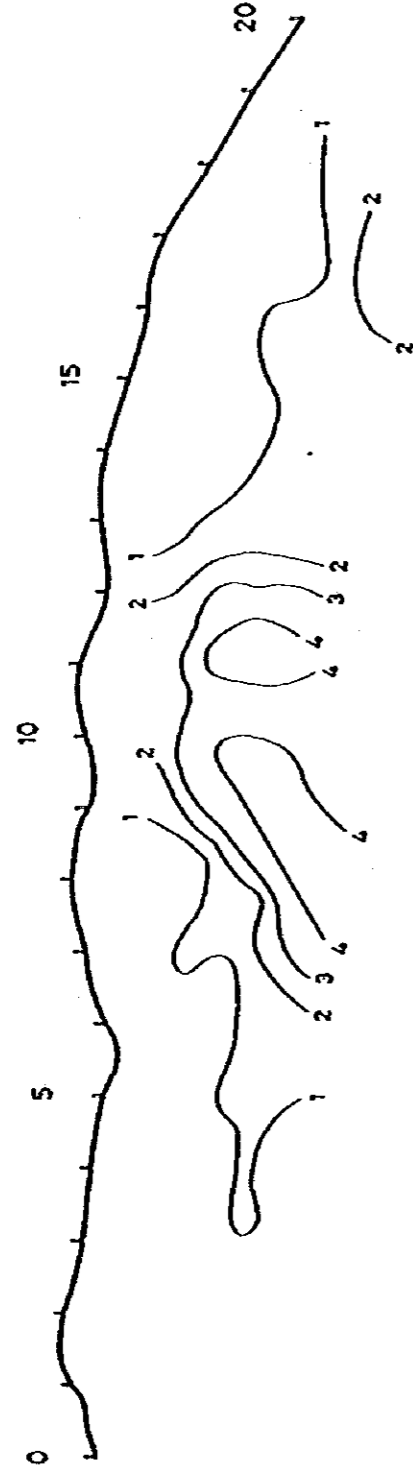


|   | $\rho$ ( $\Omega$ -m) | FE(%) |
|---|-----------------------|-------|
| 1 | 100                   | 2     |
| 2 | 50                    | 2     |
| 3 | 10                    | 15    |
| 4 | 10                    | 2     |

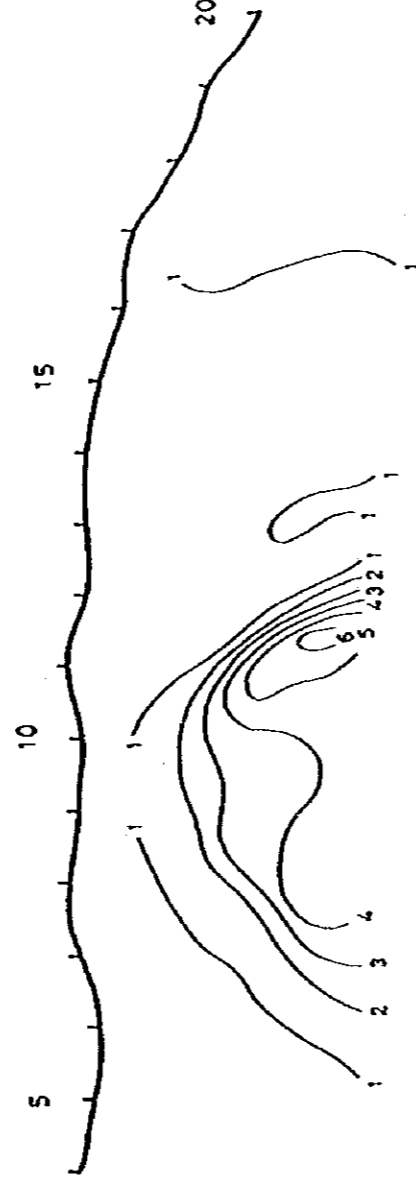
Results of Simulation Analysis for Line - E4

Scale 1:10000

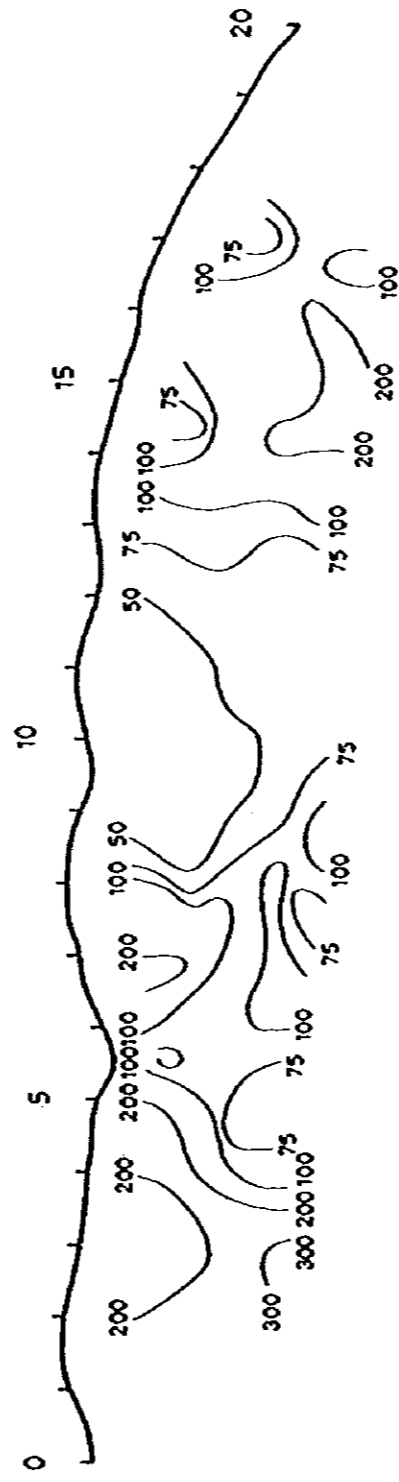
Field Data of FE(%)



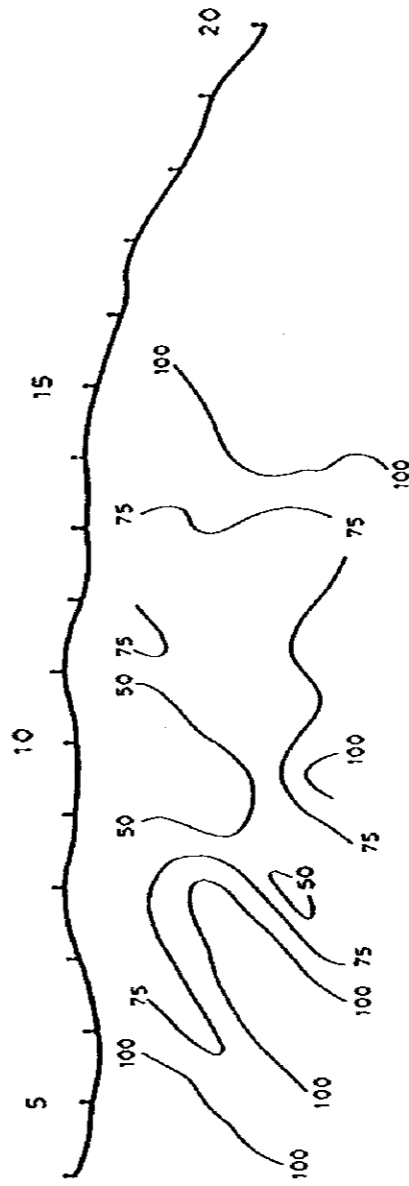
Simulation Result(%)



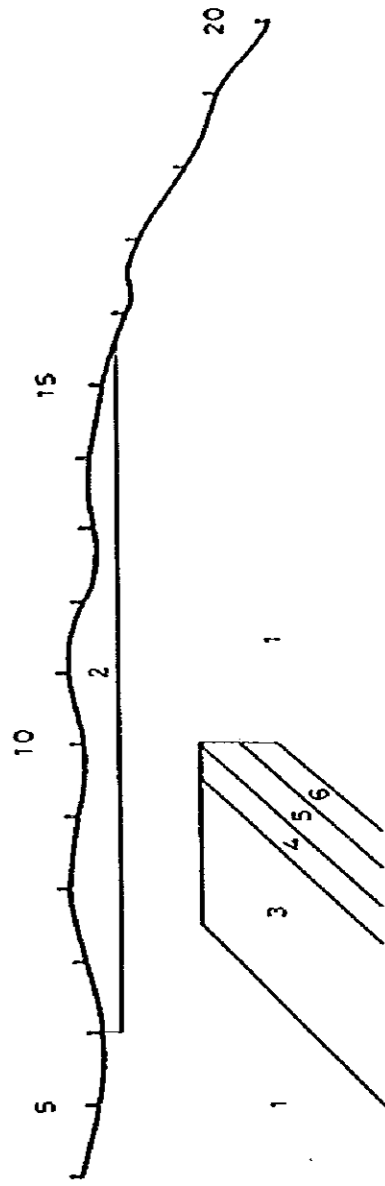
Field Data of Apparent Resistivity( $\Omega$ -m)



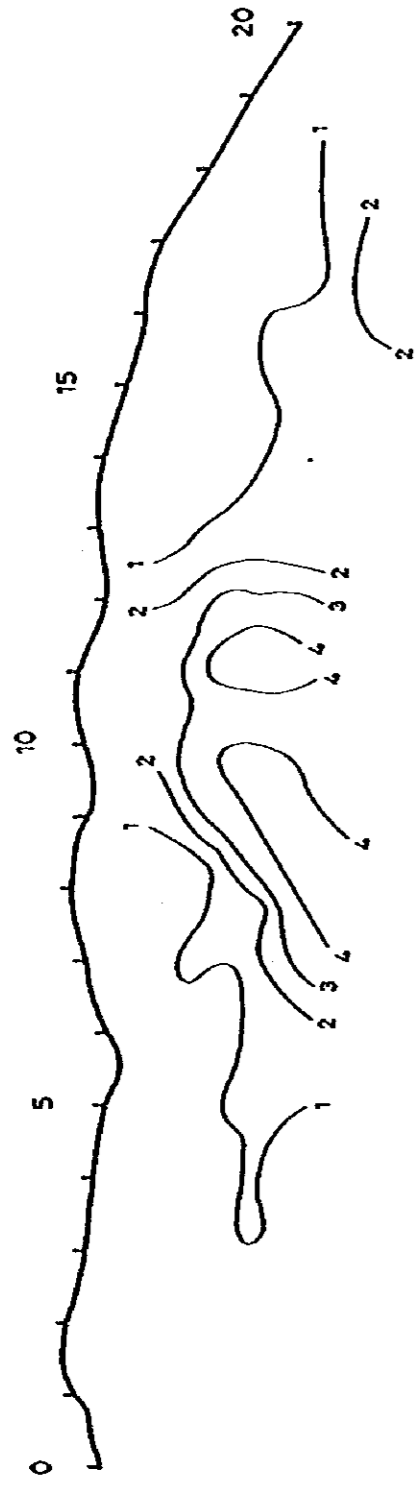
Simulation Result( $\Omega$ -m)



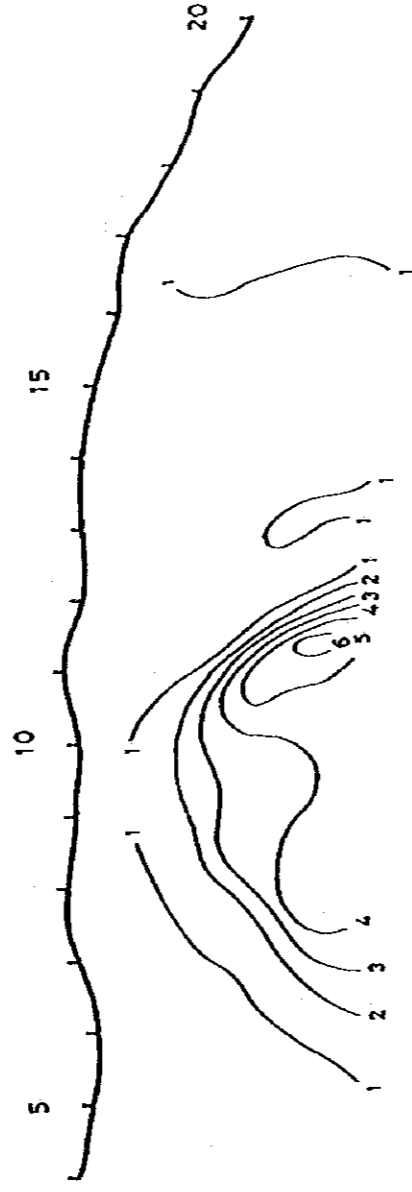
Coded Simulation Model



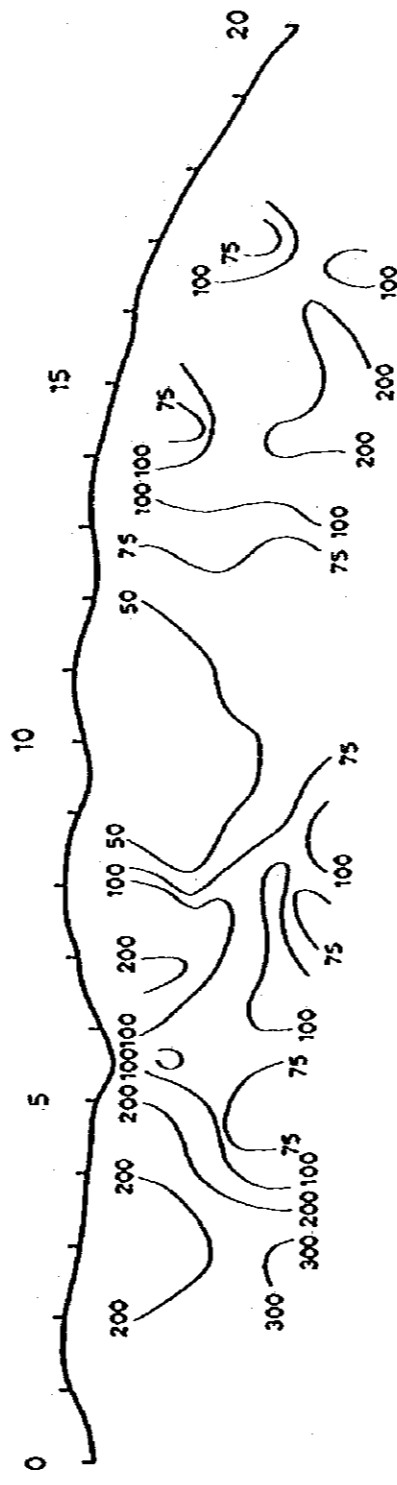
Field Data of FE(%)



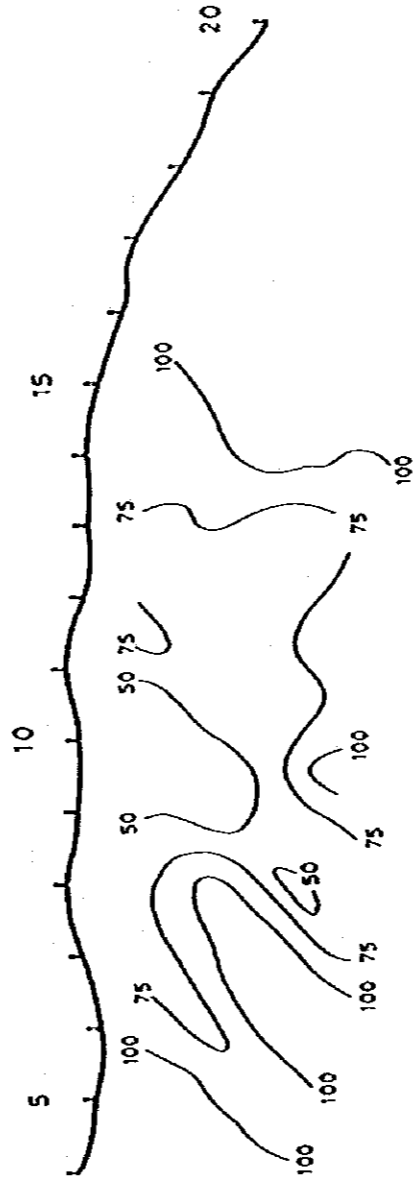
Simulation Result(%)



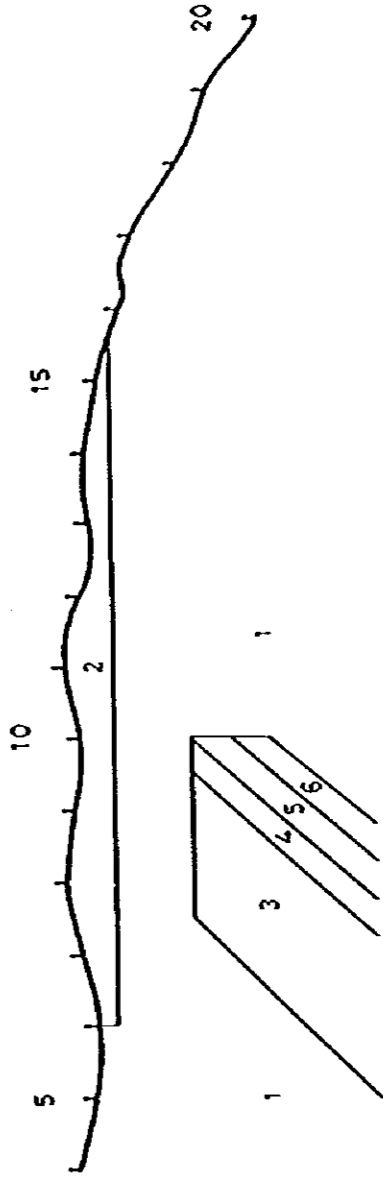
Field Data of Apparent Resistivity( $\Omega$ -m)



Simulation Result( $\Omega$ -m)



Coded Simulation Model



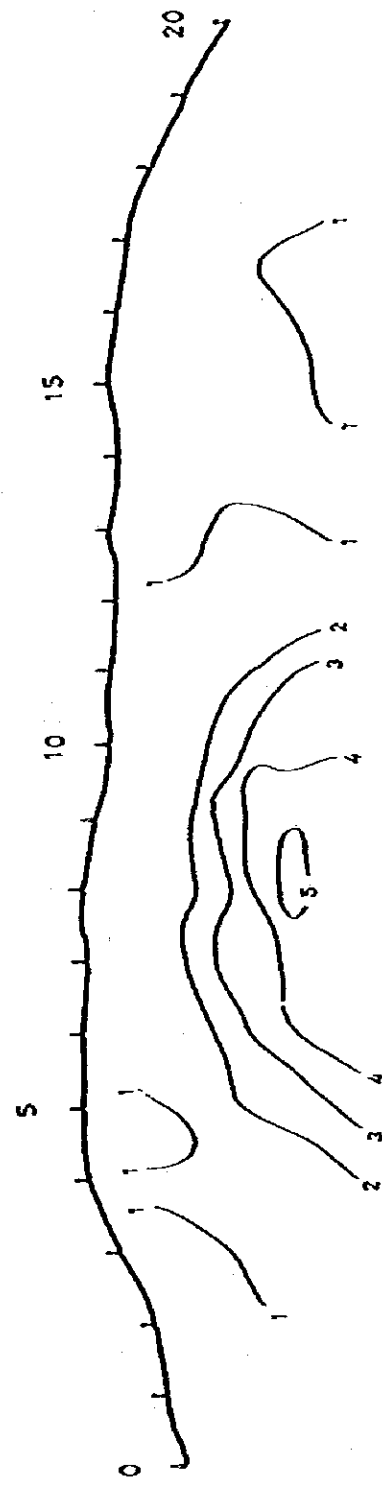
|   | $\rho(\Omega\text{-m})$ | FE(%) |
|---|-------------------------|-------|
| 1 | 100                     | 1     |
| 2 | 30                      | 1     |
| 3 | 200                     | 1     |
| 4 | 200                     | 5     |
| 5 | 10                      | 20    |
| 6 | 10                      | 1     |

Fig. 27

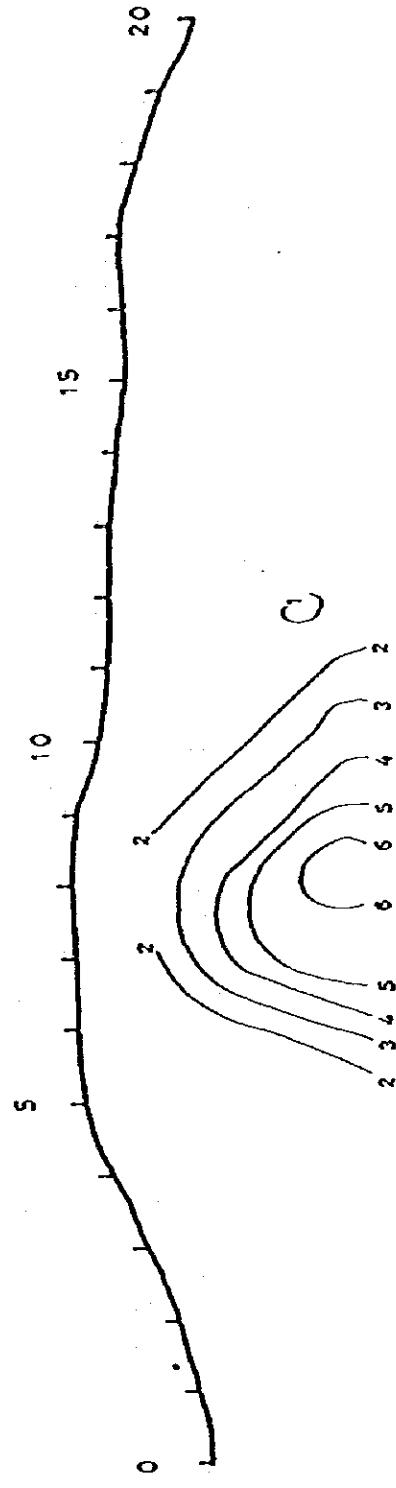
Results of Simulation Analysis for Line - E12

Scale 1:10000

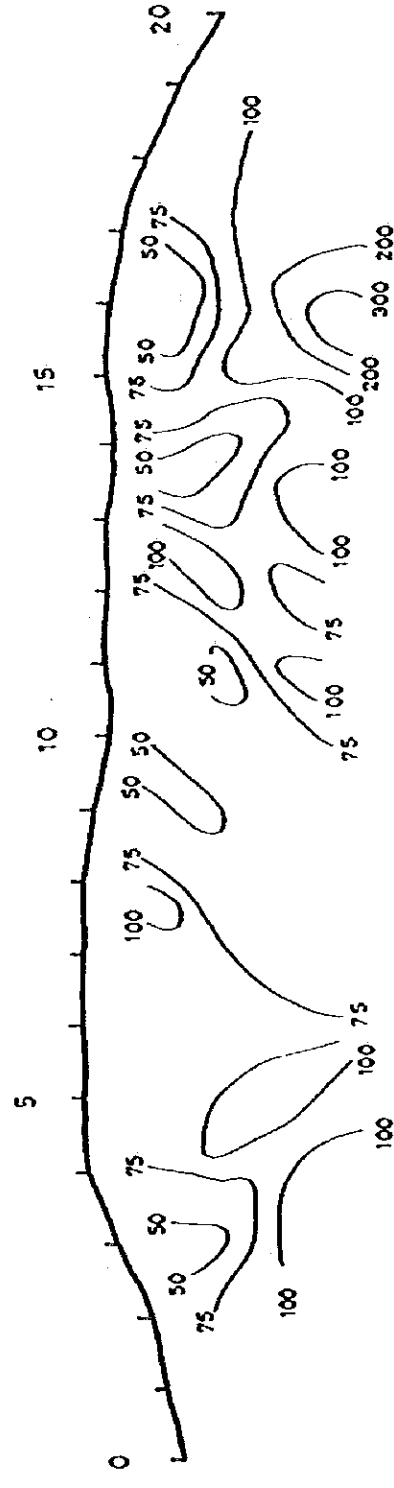
Field Data of FE (%)



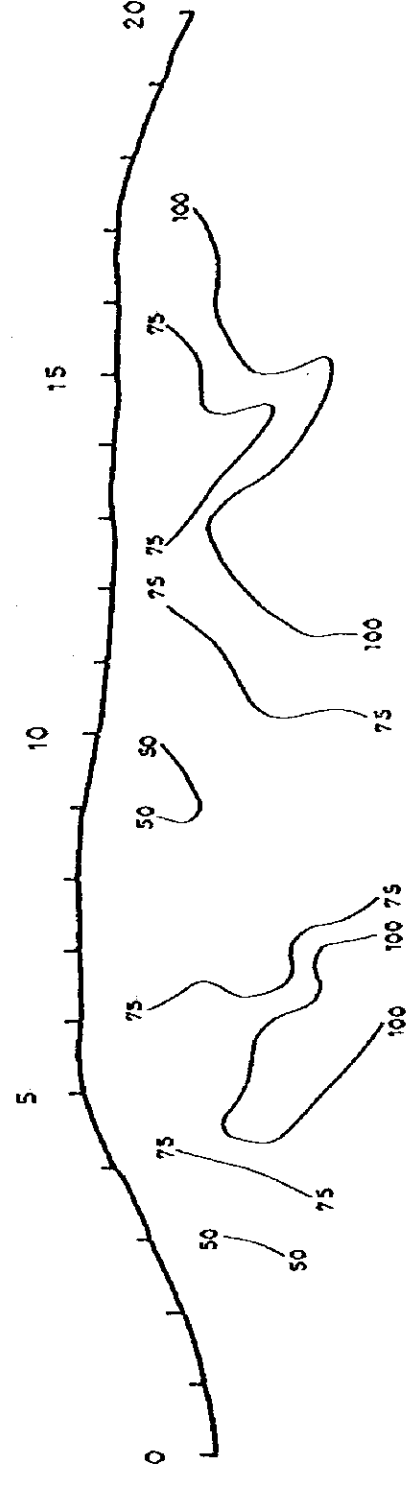
Simulation Result (%)



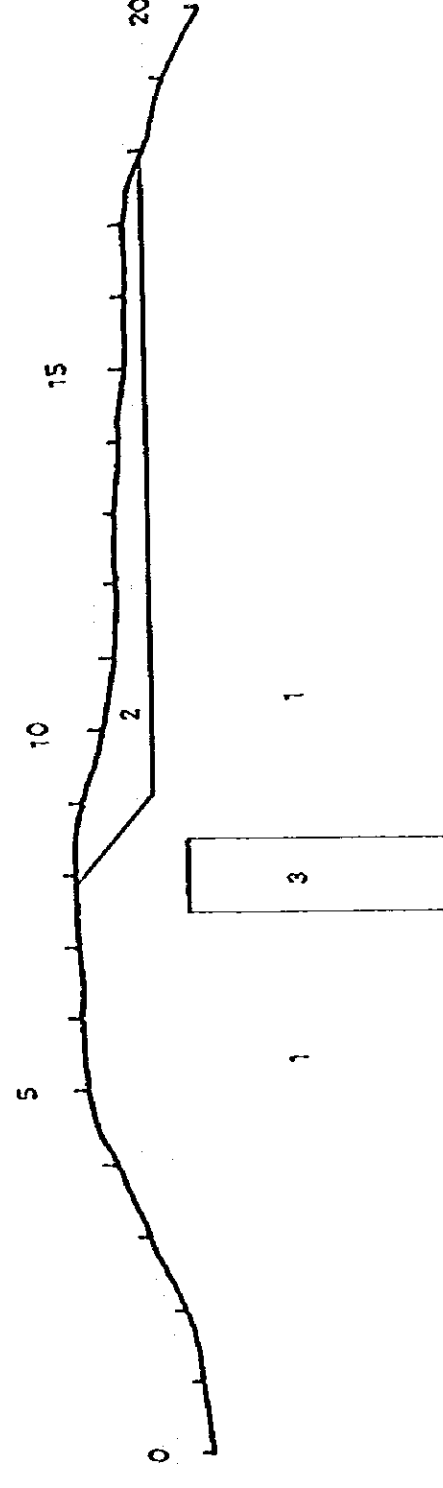
Field Data of Apparent Resistivity ( $\Omega$ -m)



Simulation Result ( $\Omega$ -m)

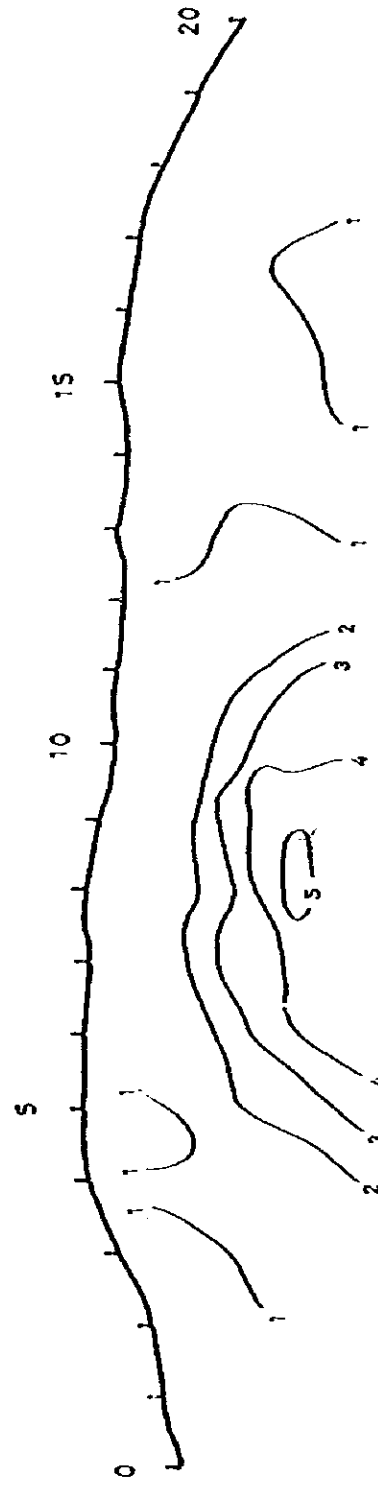


Coded Simulation Model

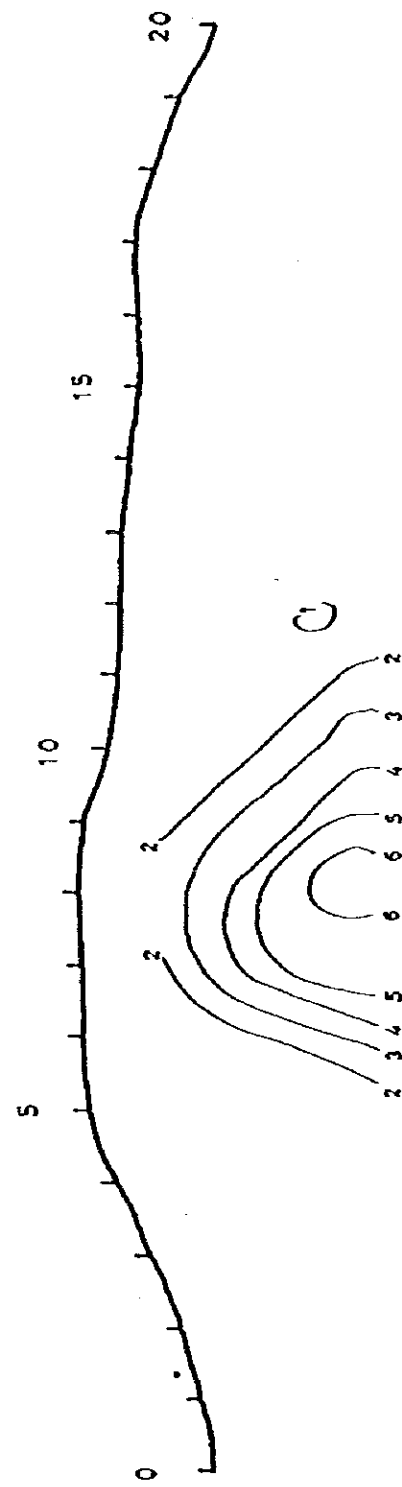


|   | $\rho(\Omega\text{-m})$ | FE (%) |
|---|-------------------------|--------|
| 1 | 100                     | 2      |
| 2 | 50                      | 2      |
| 3 | 10                      | 20     |

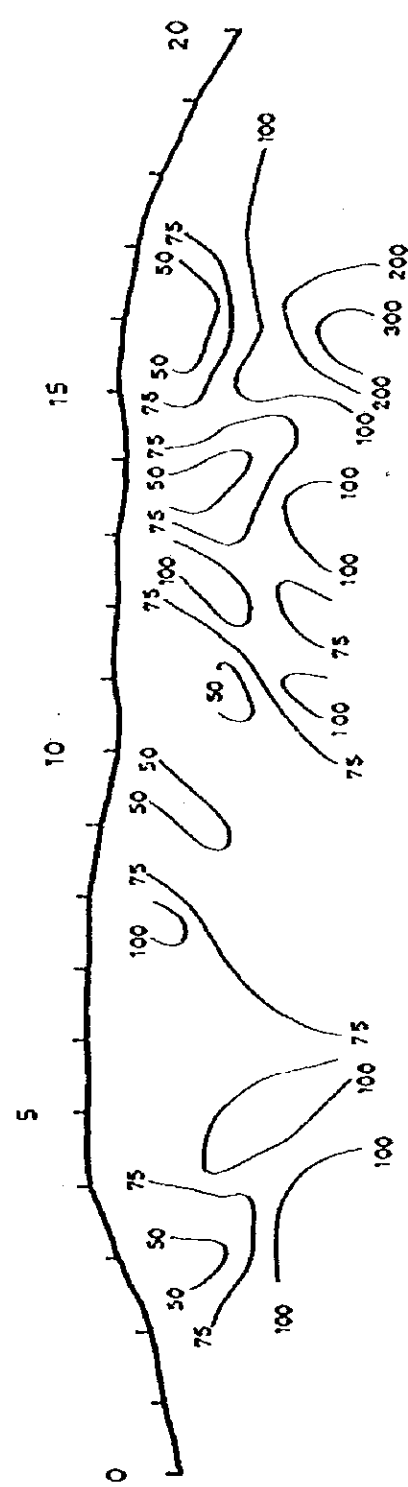
Field Data of FE (%)



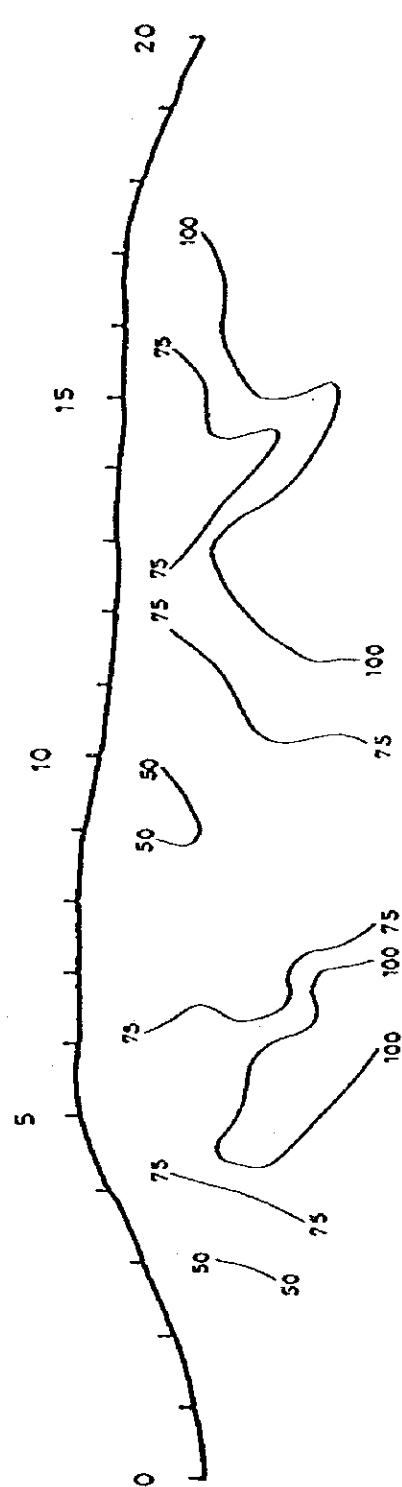
Simulation Result (%)



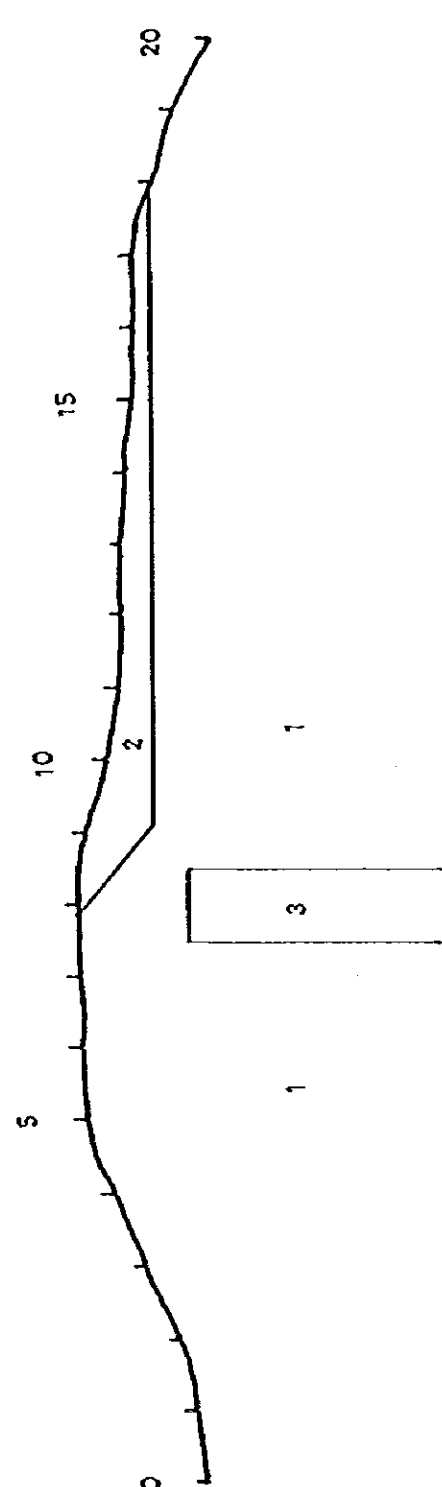
Field Data of Apparent Resistivity ( $\Omega$ -m)



Simulation Result ( $\Omega$ -m)



Coded Simulation Model



|   | $\rho(\Omega\text{-m})$ | FE (%) |
|---|-------------------------|--------|
| 1 | 100                     | 2      |
| 2 | 50                      | 2      |
| 3 | 10                      | 20     |

Line-0(Fig.25):The ore body model is a southward dipping model, having FE and AR values of 2% and 500 $\Omega$ -m, respectively, top of which is centered in the vicinity of station 10. A 100 $\Omega$ -m AR layer with 2% FE is distributed on the south side of this ore body model and a 10 $\Omega$ -m low AR layer with 2% FE on the north side. Farther to the north of this low AR layer, a layer having the same properties with that of the south side layer is widely distributed. Near the surface a 10 $\Omega$ -m low AR layer with 2% FE is assumed to exist. The top of the ore body is approximately 60m below the ground surface.

Line-E4(Fig.26): The ore body model comprises two kinds of southward dipping high FE zones which have FE values of 5% and 20%, and resistivity values of 200 $\Omega$ -m and 10 $\Omega$ -m respectively. The model has a top centered in the vicinity of station 10, and is accompanied with high resistivity part at the hanging wall side and low resistivity part at footwall side. All of these occur in a layer with 1% FE and 100 $\Omega$ -m resistivity. A 30 $\Omega$ -m low AR layer with 1% FE is assumed to exist near the ground surface. The top of the model is approximately 150m below the surface.

Line-E12(Fig.27): The ore body model, existing in a 100 $\Omega$ -m AR layer with FE value of 2%, is a vertical vein-like one centered in the vicinity of station 8. FE and AR values of the model are 20% and 10 $\Omega$ -m. A 50 $\Omega$ -m AR layer with FE value of 2% is assumed to exist near the ground surface. The top of the model is approximately 150m below the surface.

#### 5-4 Ground magnetic survey

The ground magnetic survey was carried out, as outcrops and floats of massive magnetite are widely observed here and there on the surface of the investigated area. The picket lines for IP measurements and geochemical sampling were utilized for the magnetic measurements. A magnetometer Geometrix G-819 was used for the measurements with an accuracy of  $\pm 1$  gamma.

The detail of the survey is described in p.217-221 in the Phase-II report. The distribution of magnetic field is shown in PL-98 of the same report, and the result of the analysis in PL-99, respectively. The projection of the magnetic anomalies on -150m level plan (n=3 in IP) is shown in Fig.23 in this report, as well as IP anomalies.

#### 5-4-1 Results of measurement

The magnetic intensity varies from 40,640  $\gamma$  to 42,980  $\gamma$  with a range of 2,340  $\gamma$  in the investigated area. The range is rather large, compared with the extent of the area. However, the most of the values distribute between 40,800 and 40,900  $\gamma$ . General trend of the isogram is nearly parallel to the base line, extending in the WNW-ESE direction, but a local trend in the EW direction is also observed in some places.

Two major groups of anomalies were located within the investigated area; one is in the central part, and another is in the northern part near to the limit of the area.

The central one occurs approximately along the base line, and is characterized by following natures; (1) its low anomalies have an wide areal extent, (2) its high anomalies have high-amplitude, and (3) the change rate from the high to low is large.

The northern one is located just north of the low anomalies of the central group. Its high anomalies are distributed in an area from the station-16 on line W-14 to the station-20 on line E4. However, its paired low anomalies are distributed to the north, outside of the investigated area.

#### 5-4-2 Results of interpretation

The located two groups of anomalies were interpreted to be attributed to the magnetic bodies of vein-like form. The central group comprises the anomalies elongated in the WNW-ESE, and is apparently divided into four blocks by three inferred faults. These anomalies were interpreted to be derived from a magnetic body, which was 100m to 300m wide and had the magnetic susceptibility of  $1.0 \times 10^{-3}$  emu/cc, and the top of which was from 60 to 100m deep from the surface. The magnetic body was inferred to dip steeply to the south in most places, but to the north between W8 and 0.

The northern group was interpreted to be attributed to a magnetic body which extended in EW direction, and dipped vertical to slightly to the north. Its top depth was inferred to be about 70m from the surface. It was also anticipated to have a width around 70m, and magnetic susceptibility of some  $1.4 \times 10^{-3}$  emu/cc.

These magnetic bodies were interpreted in the Phase-II report to be derived from magnetite rich-mineralization, since the susceptibility of



more than 70% of handspecimens collected from the surface had indicated less than  $0.2 \times 10^{-3}$ .

## 5-5 Discussion

Diamond drilling was carried out in the geophysical anomalies located in the Phase-II.

The drills in the IP anomalies have revealed that the IP anomalies are attributed, without exception, to extremely pyritized zone in altered rocks including skarn. Pyritization ranges in sulfur content from several % S up to nearly 30% S, and often concentrates to form semi-massive pyrite for several-m intervals (S=some teen % to 20%). However, all the three DDHs that intersected "Z-order Zn-mineralization are located outside or at the margin of IP anomalies (Fig.23).

At present, no conclusion can be made on the applicability of the magnetic survey, as no drill has been done in the most prominent inferred magnetic body occurring between W4 and O-lines. A widely distributed anomaly, which coincides approximately with IP anomalies and includes the prominent magnetic body mentioned above, may be derived from magnetite in the pyrite zone. The magnetite seems to reach some several % as a whole, though no data to evaluate exactly the content are available.

The correlation between the geophysical anomalies and drill results is summarized in Table-16.

In the present program, IP resulted in to have indicated only strong pyritization, but not economic mineralization directly. However, it should be appreciated that IP substantiated to be useful to locate sulfides below the limonitized surface.

We consider that IP is worth applying to exploration of a deposit in which useful minerals are expected to accompany pyrite, and that it is

Table-16 Correlation between Geochemical & Geophysical Anomalies, and DDH Results (After Tables-28 in Phase-II Report)

| No        | Location (m) | Length (m) | What were originally inferred when drills were planned   |  |   |                                  |   | Summary of Results                      |  |     |           |  |
|-----------|--------------|------------|--|--|---|----------------------------------|---|---|--|-----|-----------|--|
|           |              |            | Relationship with Geology & DDHs previously carried out  | Relationship with Geochemical Anom.  | Relationship with Geophysical Anom. at -150mL | PE                               | AR                                      |   | MCF  | Mag | IP Simul. |  |
| MJ-1      | X 691.042    | 258.3      | To Explore expected deeper extension of sub-economic intersection in UN-4 by UN  |  |   |                                  |   |   |  |     |           | No conspicuous mineralization at depth. only oxide min. 40.0-45.9m (5.9m) Ag 8.4g/t Zn 1.42% |
|           | Y 1693.660   |            |  |  |   |                                  |   |   |  |     |           |  |
| MJ-2      | X 691.137    | 300.1      | At inferred quartz porphyry-meta sediment contact  | To confirm deeper extension of Cu anomaly by UN  | in Phase-II                                   |                                  |   |   |  |     |           | Only intersected quartz porphyry   |
|           | Y 1693.775   |            |  |  |   |                                  |   |   |  |     |           |  |
| MJ-3      | X 690.116    | 272.3      |  | To confirm a conspicuous IP anomaly by UN  |   |                                  |   |   |  |     |           | Semi-massive Pyrite intersected 104.5-110.5m (6m) AS 5.6R/E S 16.13% Zn 0.10% Fe 34.6%       |
|           | Y 1693.998   |            |  |  |   |                                  |   |   |  |     |           |  |
| MJ-4      | X 689.958    | 150.2      | In the vicinity of granitic dyke(?) - altered sedimentary rocks contact. To explore deeper extension of geochemical & Zn anomalies at both sides of a mylonite.                          | On axis of a syn-cline, at both sides of which Cu & Zn anomalies occur.                    | Within anomaly (AR275m) (MCF240)              | Within anomaly (AR275m) (MCF240) | Within inferred magnetic body.          | Within inferred magnetic body.          | Within inferred mineralized body by simul. |     |           | 84.5-150.2m Py-Zone 92.7-98m (5.3m) Cu 0.03% S 14.5% Zn 0.22% Fe 18.5%                       |
|           | Y 1694.023   |            |  |  |   |                                  |   |   |  |     |           |  |
| MJ-5      | X 690.113    | 151.3      | To explore southern extension of the skarn zone intersected in MJ-3 (oxidized skarn at 41.75-54.57m & 104.5-110.5m)  | To explore southern -deep extension of Cu, Pb, Zn anom. at around E2-4, Station Nos. 13-14 | "   | "                                | At periphery of inferred magnetic body. | At periphery of inferred magnetic body. | -  |     |           | 116.4-121.9m (4.9m) Ga, Skarn, Mc-Py.  |
|           | Y 1693.927   |            |  |  |   |                                  |   |   |  |     |           |  |
| MJ-6      | X 690.848    | 150.8      | To explore geochem. anomalies mentioned in the right column, which occur at both sides of a quartz porphyry dyke, at the southern side.  | To explore deeper extension of Cu-Pb-Zn & Cu-Zn anomalies.                                 | About 100 to 150m outside of anomalies.       |                                  |   |   |  |     |           | 29.3-57.3m only weak Mc. imp. in Q-Porph.  |
|           | Y 1694.009   |            |  |  |   |                                  |   |   |  |     |           |  |
| MJ-7      | X 690.260    | 300.1      | To explore expected 3 horizons of skarns at their granitic contact.  | Not directly related with nearby anomaly.  | Within anomaly (AR275m) (MCF240)              | Within anomaly (AR275m) (MCF240) | At periphery of inferred magnetic body. | At periphery of inferred magnetic body. | Within inferred mineralized body by simul. |     |           | Granite between 84.1-118.7m, 124.5-128.8m (4.3m) Chl.-Diop.-Ep.-Ga. Skarn with Py. -Net      |
|           | Y 1693.890   |            |  |  |   |                                  |   |   |  |     |           |  |
| MJ-8      | X 690.400    | 150.2      | To explore the geochemical anomaly mentioned in the right column at around quartz porphyry contact.  | To explore northern -deep extension mentioned above.                                       | About 50 to 100m outside of anomalies.        |                                  |   |   |  |     |           | No conspicuous mineralization  |
|           | Y 1694.198   |            |  |  |   |                                  |   |   |  |     |           |  |
| MJ-9      | X 691.075    | 150.2      | To explore southern-deep extension of sub-marginal ores intersected by UN-4 & MJ-1 between granite & UN-4. UN-4: Zn 2.96% for 5.5m-interval, MJ-3: Zn 1.82% for 1.0m & Zn 2.72% for 2.1m | Not directly related with nearby anomaly.  | About 20 to 30m outside of anomaly.           | Within anomaly (AR275m) (MCF240) | Within inferred magnetic body.          | Within inferred magnetic body.          | -  |     |           | 18.4m Ga-Ep Skarn zone 67.0-112.0m massive Py.   |
|           | Y 1693.511   |            |  |  |   |                                  |   |   |  |     |           |  |
| MJ-10     | X 690.135    | 150.2      | Same location to DC-9, in which massive Zn ore was intersected at around hole end. To explore northern extension of 2 horizons of skarn intersected by MJ-1 at well as the above.        | Within Zn anomaly  | "   | "                                | At periphery of inferred magnetic body. | At periphery of inferred magnetic body. | -  |     |           | 45.7-46.9m (1.2m) massive Hem. 53.6-60.9m (7.3m) massive Py.                                 |
|           | Y 1694.175   |            |  |  |   |                                  |   |   |  |     |           |  |
| MJ-10 (2) | Elev. 1,832  |            |  |  |   |                                  |   |   |  |     |           |  |

\*1 Non-in parentheses indicate proposed No. in Phase-II Report  
 \*2 Coordinates & Elevations are taken from 1/10,000 Topo Map.  
 Elev.: Collar Elevation

also worth applying as a supplementary tool to geochemical survey and geological mapping, when the oxide zone is deep, or when mineral zoning is expected to exist with pyrite halo.

## 6. Diamond Drilling

### 6-1 Works carried out

10 DDHs totaling 2,033.7m were carried out in Area-C Llano del Coyote in the Phase-II and -III of the present project. In the Phase-II, a drill rig Tone TGM-5A was used, and in the Phase-III two rigs the Tone and a Boyles Bros BBS-1 were used. The net drilling terms except the preparatory period, such as transportation, site-preparation, installation, etc., were as follows: In the Phase-II; from September 25, 1977 to March 11, 1978. In the Phase-III; from July 5 to October 14, 1978.

The details concerning equipments, consumables, and operation, etc. are described in the Phase-II, and -III reports, and are omitted here in this report.

Summary of drill locations and lengths is tabulated in Table-17, in which those of UN and DGMH are also included for reference. Coordinates in this table were read in the 1/10,000 photogrammetric topographic map, and were not actually chained. Drill locations are plotted in Fig.23 in 5-3-4 in this report.

### 6-2 Purpose

The purpose of 3 DDHs in the Phase-II was as follows: (1) To explore the geophysical and geochemical anomalies located by UN, at depth in order to facilitate the interpretation of the results of the geological mapping, and geochemical and geophysical surveys, which were simultaneously carried out in the same phase. (2) To explore the extension of the sub-economic intersection in UN-4 drill (5.5m, 2.96% Zn).

The purpose of the drills in the Phase-III was to explore our geophysical and geochemical anomalies located in the Phase-II, at depth.

### 6-3 Results of DDHs

DDH MJ-9 of the third phase intersected promising primary sulfide Zn-mineralization between 88.6m and 98.1m (12.76% Zn for 9.5m). The intersection is located S13°E of MJ-1 (oxide; 1.42% for 5.9m) with a horizontal distance of about 150m. MJ-9 is located S50°E from the mineralized intersection in UN-4 (sulfide; 2.96% Zn for 5.5m) with a horizontal distance of about 135m. These three intersections are in a same skarn horizon that occurs around the boundary between the Tactic and Chicol Formations.

In MJ-9, supergene chalcocite(djurleite?) was also intersected between 82.3m and 82.9m(3.80% Cu for 0.60m). Chalcocite occurs interstitial-to residual pyrite grains in limonite gossan. The intersection is situated at the lowermost part in the oxide zone.

Summary of locations and lengths of all the DDHs that have been carried out in the prospect is tabulated in Table-17. Assay results of major mineralized intersections in these holes are listed in Table-18. In these tables data of DDHs by UN and DGMH are also compiled, as long as they are available.

Table-17 Summary of Diamond Drill Holes

| DDH No. | #1        | Location #2       |                   | Collar Elevation(m) | Length (m) | Bearings | Inclination | Remarks                      |
|---------|-----------|-------------------|-------------------|---------------------|------------|----------|-------------|------------------------------|
|         |           | UTM Coordinates X | UTM Coordinates Y |                     |            |          |             |                              |
| UN-1    |           | 690.173           | 1694.055          | 1,817               | 77.78      | S40°W    | -60°        | Nov.27-Dec.27,1969 Winkle    |
| UN-2    |           | 690.328           | 1693.930          | 1,855               | 83.88      | N        | -60°        | Feb.2-Feb.27,1970 Winkle     |
| UN-3    |           | 690.353           | 1693.018          | 1,833               | 79.30      | S        | -65°        | Mar.8-Apr.24,1970 Winkle     |
| UN-4    |           | 690.043           | 1693.658          | 1,820               | 147.32     | S42°W    | -50°        | Aug.3-Aug.26,1970 Boyles     |
| UN-5    |           | 690.062           | 1693.968          | 1,860               | 114.68     | N40°E    | -70°        | Aug.29-Sept.21,1970 Boyles   |
| UN-6    |           | 691.302           | 1693.280          | 1,830               | 96.38      | S40°W    | -60°        | Sept.27-Oct.16,1970 Boyles   |
| UN-7    |           | 691.198           | 1693.117          | 1,857               | 152.20     | N40°E    | -70°        | Oct.19-Nov.17,1970 Boyles    |
| DG-8    |           | ?                 | ?                 | ?                   | 104.62     | -        | -90°        | ? Winkle                     |
| DG-9    |           | 690.122           | 1694.170          | 1,835               | 85.37      | -        | -90°        | ? Winkle                     |
| MJ-1    | Phase II  | 691.042           | 1693.660          | 1,820               | 258.3      | -        | -90°        | Sept.25-Nov.19,1977 Tone     |
| MJ-2    |           | 691.137           | 1693.775          | 1,818               | 300.1      | -        | -90°        | Nov.26,1977-Jan.27,1978 Tone |
| MJ-3    |           | 690.116           | 1693.998          | 1,825               | 272.3      | -        | -90°        | Feb.11-Mar.11,1978 Tone      |
| MJ-4    | Phase III | 689.958           | 1694.023          | 1,881               | 150.20     | -        | -90°        | Jul.5-Aug.10,1978 Tone       |
| MJ-5    |           | 690.113           | 1693.927          | 1,846               | 151.30     | -        | -90°        | Jul.11-Jul.31,1978 Boyles    |
| MJ-6    |           | 690.848           | 1694.009          | 1,831               | 150.80     | -        | -90°        | Aug.1-Aug.14,1978 Boyles     |
| MJ-7    |           | 690.260           | 1693.890          | 1,837               | 300.10     | -        | -90°        | Aug.11-Sept.25,1978 Tone     |
| MJ-8    |           | 690.400           | 1694.198          | 1,810               | 150.20     | -        | -90°        | Aug.15-Aug.29,1978 Boyles    |
| MJ-9    |           | 691.075           | 1693.511          | 1,847               | 150.20     | -        | -90°        | Aug.30-Aug.25,1978 Boyles    |
| MJ-10   |           | 690.135           | 1694.175          | 1,832               | 150.20     | -        | -90°        | Sept.26-Oct.14,1978 Boyles   |

\*1 UN-: By United Nations, DG-: By DGMH, MJ-: NMAJ-JICA/DGMH

Table-18 Summary of Mineralized Diamond Drill Intersections (1)

| DMS No. | Depth (m)     | Length (m) | Average Commin %1 |       |       |       |       | Remarks |   |
|---------|---------------|------------|-------------------|-------|-------|-------|-------|---------|---|
|         |               |            | As(%)             | Cu(%) | Pb(%) | Zn(%) | Fe(Z) |         | S(Z)  |
| MJ-1    | 9.00-10.00    | 1.00       | 15.8              | 0.09  | -     | 1.82  | -     | -       | * Common altered garnet-epidote skarn with magnetite.   |
|         | 40.00-45.90   | 5.90       | 8.4               | -     | -     | 1.42  | -     | -       | * Garnet-epidote skarn stained with limonite & manganese oxide.   |
|         | 51.70-34.20   | 2.50       | 19.4              | -     | -     | 0.21  | -     | -       | * Common with altered quartz porphyry.  |
|         | 90.60-94.00   | 3.40       | 10.4              | 0.11  | -     | -     | -     | 4.27    | * Altered rhyolite with closely spaced pyrite veinlets. Chalcosite film coating pyrite veinlets (up to 2mm wide). |
| MJ-2    | 29.70-37.60   | 4.00       | 10.3              | 0.06  | -     | -     | -     | -       | * (Garnet?) - epidote skarn stained with limonite.  |
|         | 86.50-88.00   | 1.50       | 19.3              | 0.09  | -     | -     | 20.12 | -       | * Rhyolite with partly limonitized magnetite.   |
| MJ-3    | 61.75-42.47   | 0.72       | 8.5               | 0.03  | 0.04  | 0.53  | 2.46  | -       | * Chlorite - garnet skarn stained with limonite.  |
|         | 51.66-56.68   | 4.82       | 20.4              | 0.07  | -     | 0.22  | 27.79 | -       | * Common with silicified shale or sandstone(?).   |
|         | 104.50-110.50 | 6.00       | 5.6               | -     | -     | 0.10  | 34.06 | 16.13   | * Garnet - epidote skarn with network of pyrite and magnetite.  |
| UN-1    | 27.8 - 36.6   | 8.80       | N.A               | 0.04  | -     | 0.30  | -     | -       | * Epidote-quartz rock (silicified shale with epidote) with yellow sphalerite(?).                                  |
| UN-4    | 48.90-49.40   | 0.50       | N.A               | 0.12  | 0.38  | 2.55  | -     | -       | * Altered quartz porphyry(?) stained with limonite & hematite.  |
|         | 64.05-65.05   | 1.00       | N.A               | -     | -     | 0.72  | -     | -       | * Bleached & limonitized quartz porphyry or granite.  |
|         | 73.40-76.83   | 1.43       | N.A               | 0.10  | -     | 0.37  | -     | -       | * Epidote skarn(?) stained with limonite.   |
|         | 118.95-122.0  | 3.05       | N.A               | 0.02  | 0.02  | 0.46  | -     | -       | * Epidote - chlorite skarn.   |
|         | 124.1 -129.6  | 5.50       | N.A               | 0.38  | 0.02  | 2.96  | -     | -       | * Epidote - chlorite skarn (dark green rock) with pyrite & sphalerite.  |
| UN-5    | 85.4 -100.65  | 15.25      | N.A               | 0.09  | -     | 0.23  | -     | -       | * Epidote - chlorite skarn with rubby sphalerite dissemination. In situ limonite weathered moderately.            |
| UN-6    | 74.63-78.69   | 4.06       | N.A               | 0.01  | -     | 0.21  | -     | -       | * Silicified quartz porphyry with massive pyrite at 76.36-78.17m.   |
| DG-9    | 79.67-85.17   | 5.50?      | N.A               | N.A   | N.A   | N.A   | N.A   | N.A     | * Chlorite-hedenbergite(?) skarn with massive pyrite-sphalerite ore. Poor recovery & no assay results available.  |

\* : For all "UN-Drill", arithmetic averages are calculated from assay results described in Appendix-IV in UN Report, 1973.  
 N.A.: Not analyzed.  
 --- : Average is not calculated, as value is extremely low.

Table-18 Summary of Mineralized Diamond Drill Intersections-2

| DDK No.         | Depth (m)       | Length (m)    | Assay Results |          |        |        |        |        |       |        |      |   | Remarks   |
|-----------------|-----------------|---------------|---------------|----------|--------|--------|--------|--------|-------|--------|------|---|---|
|                 |                 |               | Au (g/t)      | Ag (g/t) | Cu (%) | Pb (%) | Zn (%) | Fe (%) | S (%) | Mn (%) |      |   |   |
| MJ-4            | 64.70 - 66.30   | 1.60          | N.A.          | 2        | 0.04   | -      | -      | -      | 27.00 | -      | 0.57 | * Limonite goussan  |   |
|                 | 81.50 - 81.90   | 0.40          | -             | 2        | 0.04   | -      | -      | -      | 22.08 | -      | -    | * ditto   |   |
|                 | 92.70 - 98.00   | 5.30          | N.A.          | -        | 0.03   | -      | 0.22   | -      | 18.49 | 14.51  | -    | * Skarnized rock with dense aggregate of pyrite                       |   |
|                 | 112.00 - 114.65 | 2.65          | N.A.          | 4.4      | 0.10   | -      | 0.49   | -      | 11.64 | -      | -    | * Limonite stained part in altered rock                               |   |
|                 | 117.40 - 118.40 | 1.00          | N.A.          | 1.6      | -      | -      | 0.42   | -      | 14.20 | 8.45   | 0.69 | * Epidote rock with pyrite veinlets and disseminations.               |   |
|                 | 80.30 - 81.60   | 1.30          | N.A.          | -        | 0.07   | -      | -      | -      | 14.61 | 9.29   | -    | * Epidote rock with vein form aggregate & dissemination of pyrite.    |   |
|                 | 83.20 - 83.90   | 0.70          | N.A.          | -        | 0.07   | -      | -      | -      | 12.62 | 8.86   | -    | * ditto   |   |
|                 | 84.60 - 85.30   | 0.70          | N.A.          | -        | 0.04   | -      | -      | -      | 9.36  | 6.30   | -    | * ditto   |   |
|                 | 91.90 - 94.20   | 2.30          | N.A.          | -        | -      | -      | -      | -      | 15.76 | 15.10  | -    | * Altered rock with dense pyrite dissemination                        |   |
|                 | 100.50 - 101.10 | 0.60          | -             | -        | -      | -      | -      | -      | 16.40 | 16.67  | -    | * ditto   |   |
| MJ-5            | 116.40 - 121.30 | 4.90          | 0.55          | 1.8      | 0.03   | -      | -      | -      | 20.70 | 7.17   | -    | * Garnet-epidote rock with dense pyrite dissemination.                |   |
|                 | 130.60 - 131.30 | 0.70          | N.A.          | -        | 0.03   | -      | -      | -      | 10.39 | 4.37   | -    | * Chloritized rock with pyrite dissemination                          |   |
|                 | 15.00 - 18.90   | 3.90          | N.A.          | -        | 0.05   | -      | -      | -      | -     | -      | -    | * Limonite goussan  |   |
|                 | 75.60 - 75.80   | 0.20          | N.A.          | -        | 0.02   | -      | -      | -      | 13.38 | 13.34  | -    | * Fault gouge with sporadic pyrite dissemination.                     |   |
|                 | 81.60 - 82.75   | 1.15          | N.A.          | 2        | 0.09   | -      | -      | -      | 20.22 | 9.95   | -    | * Chlorite-epidote skarn with dense aggregate of pyrite and magnetite |   |
|                 | 84.10 - 85.00   | 0.90          | N.A.          | -        | -      | 0.05   | -      | -      | -     | 3.66   | -    | * Granitic rock with galena dissemination                             |   |
|                 | 122.30 - 127.00 | 4.70          | N.A.          | -        | -      | -      | -      | -      | 18.11 | NAV    | -    | * Chlorite-tremolite-garnet skarn with magnetite and pyrite           |   |
|                 | 187.90 - 193.40 | 2.90          | -             | -        | 0.01   | -      | -      | -      | 12.41 | NAV    | -    | * Magnetite-pyrite stringers or net-works in epidote skarn            |   |
|                 | MJ-9            | 54.70 - 54.80 | 0.10          | -        | 4      | 2.20   | -      | -      | -     | 22.02  | NAV  | -   | * Massive & semi-massive pyrite   |
|                 |                 | 82.30 - 82.90 | 0.60          | 1        | 3.80   | -      | 0.80   | -      | -     | 34.32  | NAV  | -   | * Massive limonite with chlorite (djurleite?) interstitial to relic pyrite. |
| 88.60 - 98.10   |                 | 9.50          | -             | 4        | 0.19   | -      | 12.76  | -      | 23.06 | NAV    | -    | * Garnet-chlorite skarn with densely disseminated phaladite.          |   |
| 98.10 - 107.00  |                 | 8.90          | -             | 2        | 0.04   | -      | 0.64   | -      | 22.89 | NAV    | -    | * Chlorite-epidote-garnet skarn with pyrite & sphalerite.             |   |
| 138.40 - 146.60 |                 | 3.70          | -             | 2        | 0.08   | -      | 0.35   | -      | 20.88 | NAV    | -    | * Garnet-epidote-actinolite-tremolite skarn with pyrite.              |   |
| MJ-10           | 10.40 - 11.90   | 1.50          | N.A.          | 2        | 0.02   | -      | 0.63   | -      | 8.62  | NAV    | 1.14 | * Epidotized rock with limonite stain                                 |   |
|                 | 45.70 - 49.90   | 4.20          | N.A.          | -        | 0.03   | -      | 0.22   | -      | 29.12 | NAV    | -    | * Massive hematite (after massive magnetite?)                         |   |
|                 | 53.60 - 63.90   | 9.30          | N.A.          | -        | -      | -      | -      | -      | 26.55 | NAV    | -    | * Semi-massive pyrite-magnetite with 2ndary hematite.                 |   |

N.A.: Not assayed.

NAV : Not available.

- : Average is not calculated, as value is extremely low.



However, in the sulfide zone, Zn is assayed only at 0.1% or less, and no intersection in which sphalerite occurs concentratedly has been encountered.

Supergene chalcocite, coating pyrite veinlets, was observed just below the oxide zone in MJ-1, but the 3.4m intersection is only assayed at 0.11% Cu.

In Table-18, assay results of the DDHs by both UN and DGMH are also compiled, so long as their data are available.

## 7 Conclusion and Recommendation

### 7-1 On the exploration potential of the project areas

#### 7-1-1 General

Metallic (especially non-ferrous) metallic mineralization is very weak in the project areas. This may be attributed to the fact that there is very little acidic intrusive occurrence in the areas. We conclusively consider that there remains little possibility that a metallic deposit with mineable reserves of say  $n \times 10^6 T$  or more occurs in the areas.

We guess that only mineralization types that have still some possibility of yielding small scale operating mines in future are skarn-to-hydrothermal replacement type (Cu-Zn), Pb-Zn mineralization in the Paleozoic carbonate rocks, and massive chromite in peridotite.

#### 7-1-2 (Cu-Zn) Skarn-to-Hydrothermal replacement type

This is the mineralization to which our drilling program has been concentrated. As a result, promising Zn-mineralization was intersected in DDH MJ-9 (12.76% for 9.5m). Zn-anomalies of rock-chip samples delineated by 500ppm well correlate to "Zn-order Zn-mineralized intersections" of DDHs. The anomalies have an extent of 3.6km by 0.2km as a whole, and are mostly unexplored except 4 DDHs. Therefore, possibilities that reserves of  $n \times 10^5 T$  to  $n \times 10^6 T$  exist in the prospect are considered to be fairly great. A deposit may be exploitable even this size, if Zn grade is as high as that of MJ-9, since the prospect is favorably located to minimize expenditures for infrastructures. Further exploration is warranted, and an intensive DDHs program is recommended to undertake. Proposed program is described in Phase-III Report (6-5, PL-1-1).

#### 7-1-3 Pb-Zn mineralization in carbonate rocks

Pechac, Laurita, Saclecán, and Peña de Plata are the showings of this type. However, only one that was detected as a conspicuous geochemical anomaly is "Peñasco-Pacumal anomaly" in the Pechac-Laurita area.

We consider that there still remains the possibility that high grade bonanzas may locally exist somewhere in these showings or elsewhere. However, we also infer that their dimension might be of the order of  $10^4 T$  at most, if any. As most of

*continue to next page*

the anomalies and showings of this type are located in remote areas where the infrastructure is poorly provided. We consider that it might be very difficult, if not impossible, to exploit these deposits in near future, even if some high grade small bonanzas occurred. Therefore, we believe that the exploration priority to this type in the project areas is fairly low, and that whether additional exploration is needed or not should be judged when the reconnaissance to all the other possible fields in Guatemala has been completed.

#### 7-1-4 Chromite ore in ultrabasic rocks

Massive chromite ores are often observed in the small intrusive bodies of serpentinized peridotite that occur intermittently along the fault zone of the Chixoy-Polochic fault. Though there is no known showing that warrants commercial production in near future, we could not either deny the possibility of small new ore bodies. Nevertheless, we infer that the dimension of such deposits is small, because, if a sizable deposit occurred near the surface, either outcrops or floats could have been discovered, as little vegetation is on the surface of the serpentinite exposures. We speculatively guess that the dimension of an ore deposit, if it should be discovered, would probably be of  $n \times 10^3 T$  or smaller. Therefore, the deposit would be the one which could be mined by local people as a side business when the market price rose.

#### 7-2 On selection of further target areas in Guatemala

Our present study has revealed that the non-ferrous metallic mineralization is likely related with the acidic intrusive rocks of the later Cretaceous to Paleogene. Though this relationship could not directly be applied further to other areas in Guatemala, it must be necessary to pay attention to the relationship between the mineralization and acidic intrusives. We suggest to give better exploration priority to an area, where acidic intrusives (especially those from the Cretaceous to the Paleogene in age) abundantly occur, when a regional reconnaissance for non-ferrous metallic minerals is planned in Guatemala.

#### 7-3 On exploration methods

##### 7-3-1 Geochemical survey

Through the exploration works of the present program, we have reconfirmed that geochemical survey of stream sediments and/or soil is the most

usefull exploration tool throughout all the stages from the reconnaissance to the scout drills.

As to the indicators: Three elements Cu,Pb and Zn were adopted as indicators in the Phase-I, and Ag was added to the three in the Phase-II. It is recommended to add at least Au in a further program in other areas, so far as the exploration for non-ferrous metals is concerned. For gold analysis of the exploration purpose, AAS technique with solvent extraction should be applied. It is further recommended to select carefully the most effective indicators and/or path finders in accordance with the objective metals and the geology of the target areas, when an exploration program is planned.

As the statistical technique in the geochemical data processing, the rolling mean analysis was very much useful, especially in the reconnaissance phase. Of the technique, the standard deviation highs well indicated the presence of the mineralized parts. Therefore, it is recommended to apply this technique in the reconnaissance stage of a further project. To the determination of the dimension of a search area in the rolling mean analysis, it is suggested to study the possibility of applying the variogram in the Krigging method.

To the determination of the threshold values, it may be more adequate to apply the rolling mean analysis. The procedure may be suggested as follows: To construct a surface showing "rolling mean + 2 standard deviations calculated from all the samples falling in that search area", and to define the threshold values as that surface itself.

### 7-3-2 On geophysical survey

IP anomalies tend to be attributed to pyritization, as in the case of Llano del Coyote. Also, they are often derived from underground water, zones of argillized zone, and many other causes other than mineralization. Thus, IP cannot be a unique exploration tool that detects directly useful metals, from its inherent nature.

Though IP has many weak points mentioned above, it is still helpful and applicabile in some cases as follows: It is worth applying to the exploration of a deposit in which useful minerals are expected intimately accompany pyrite. It is also applicabile as a supplementary tool to geochemical exploration and geological interpretation in the cases when leached capping, or mineral zoning is expected to occur.

In these cases, IP is recommended to apply in the stage after the reconnaissance and directly before the scout drilling.

## References

- Agnós, W.B. (1958)  
Result of airborne magnetometer profile from Brownsvilles, Texas to Guatemala City: *Geophysics* v.23, No.4, p.726-737
- Anderson, T.H. (1968b)  
Pre-Pennsylvanian and later displacements along Chixoy-Polochic fault trace, northwestern Guatemala: *Geol. Soc. America Abs. for 1968, Spec. Paper 121*, p.6
- \_\_\_\_\_, et al (1973)  
Geology of the Western Aitos Cuchumatanes, Northern Guatemala: *Geol. Soc. America Bul.* v.84, p.805-826
- Blount, D.N. (1967)  
Geology of the Chiantla quadrangle, Guatemala (Ph.D. dissrt.): Baton Rouge, Louisiana State Univ. 135p.
- Bohnenberger, O.H. (1966a)  
Nomenclatura de las capa Santa Rosa en Guatemala: *Publicaciones Geológicas del ICAITI, Guatemala, No.1*, p.47-51
- \_\_\_\_\_. (1966b)  
Liberto guía de la excursión "A", Liberto guía de las excursiones, Segunda Reunión de Geólogos de America Central: Guatemala, Ciudad de Guatemala, 151p.
- Bonís, S.B. (1967)  
Excursion Guide Book for Guatemala: Instituto Geográfico Nacional, *Geol. Bul. No.4*
- \_\_\_\_\_, Bohnenberger, O.H., and Dengo, G. (1970)  
Mapa Geológico de la Republica de Guatemala: Guatemala, C.A. Inst. Geográfico Nacional de Guatemala; 1/500,000
- Dahlberg, E.C. and Keith, M.L. (1966)  
Distribution of Trace metals in modern stream sediments from three geologically different terranes (abst.): *Geol. Soc. of Am. Special Paper 101*, p.48
- Dahlberg, E.C. (1967)  
A multivariate study of some aspects of Trace metals in stream sediments as guides to locating mineral deposits: Ph. D. Thesis, Pennsylvania State University, p.163
- \_\_\_\_\_. (1968)  
Application of a selective simulation and sampling technique to the interpretation of stream sediment anomalies near South Mountain, Pennsylvania: *Econ. Geol.* v.63, p.409-417
- \_\_\_\_\_. (1969)  
Use of model for relating geochemical prospecting data to geological attributes of a region, South Mountain, Pennsylvania: *Quarterly of the Colo. Sch. of Mines* v.64, No.1, p.195-216.
- Dengo, G. (1968)  
Estructura geológica, historia tectónica y morfología de America Central: ICITI

- Dengo, G. and Bohnenberger, O.H. (1969)  
Structural development of northern Central America in tectonic relations of northern Central America and the western Caribbean: Am. Assoc. Petroleum Geologist Mem. 11, p.203-220
- Dirección General de Minería e Hidrocarburos (1965)  
Nómina de Muestras Mineralés de Guatemala
- Garrett, R.G., and Nicol, I. (1969)  
Factor analysis as an aid in the interpretation of regional geochemical stream sediment data: Quarterly of the Colo. Sch. of Mines, v.64, No.1, p.245-264
- ICITI (1969)  
Trabajos Técnicos Presentados en la Segunda Reunión de América Central
- Instituto Geográfico Nacional de Guatemala (1968?)  
Unpublished geologic map Nebáj quadrangle; 1/50,000  
\_\_\_\_\_(1961-1962)  
Diccionario Geográfico Nacional de Guatemala  
\_\_\_\_\_(1976)  
Atlas Hidrológico (primera edición)
- Kesler, S.E. and Ascarrunz, K. (1973)  
Lead-Zinc mineralization in carbonate rocks, Central Guatemala: Econ. Geol. v.68, p.1236-1274
- Koch, A.J. and McLean, H. (1975)  
Pleistocene tephro and ash-flow deposits in the volcanic highlands of Guatemala: Geol. Soc. Am. Bul.
- Krige, D. (1951)  
A statistical approach to some mine valuation and allied problems on the Witwatersrand; M.Sc. thesis, University of the Witwatersrand
- Lepeltier, C. (1969)  
A simplified statistical treatment of geochemical data by graphical representation Econ. Geol. v.64, p.538-550
- Matheron, G. (1963)  
Principles of Geostatistics; Econ. Geol. v.58, p.1246-1266  
\_\_\_\_\_. (1971)  
The theory of regionalized variables and its applications: Cahiers du Centre de Morphologie Mathématique de Fontainebleau v.5
- McBirney, A.R. (1963)  
Geology of a part of the Central Guatemalan Cordillera
- McRee, D.E. (1969)  
Paleozoic stratigraphy and structural geology of Nebáj quadrangle, Guatemala (M.S. thesis): Baton Rouge, Louisiana State Univ., 67p.
- Mining Mission to Central American Countries (1970)  
Report on mining activity in General American Countries (in Japanese)  
Metal Mining Agency of Japan
- NSAJ/JICA (1977)  
Report on geological survey of Cuchumatanes Area, Western Guatemala (Japanese and English)

- OMAJ/JICA(1978)**  
Report on geological survey of Cuchumatanes Area, Western Guatemala  
(Japanese and English)
- Nichol, I., Garret, R.C. and Webb, J.S. (1969)**  
The role of some statistical and mathematical methods in the interpretation of regional geochemical data: Econ. Geol., v.64, p.204-220
- Roberts, R.J., and Irving, E.M. (1957)**  
Mineral deposits of Central America: U.S. Geol. Survey Bul. 1034, 205p.
- Rose, A.W., Dahlberg, E.C. and Keith, M.L. (1970)**  
A multiple regression technique for adjusting background values in stream sediment geochemistry: Econ. Geol. v.65, p.156-165
- Rosenfeld (1977)**  
Unpublished DGMH internal report: Afloramiento mineralizado, Barillas, Huehuetenango, Guatemala
- United Nations (1968)**  
Guatemala, Mineral Surveys in Two Selected Zones  
(1969-1970?)  
Unpublished internal reports for follow-up works of the mineral survey
- (1971)  
Metal mining in Guatemala, Study of old mines and abandoned prospects, Mineral Survey in Two Selected Areas
- (1973)  
Llano del Coyote --- Anomalia geoquímica No.10 ---, Informe tecnico